Zoological Journal of the Linnean Society, 2026, **207**(4), zlag124
https://doi.org/10.1093/zoolinnean/zlag124
Original Article

OXFORD

Genetic, morphological, and bioacoustic assessments of species limits in the greater African roundleaf bats, *Macronycteris* (Hipposideridae)

Daniela M. Rossoni[1,2,*], Terrence C. Demos[2,*], Paul W. Webala[3], Laura Torrent[4,5], Michael Bartonjo[6], Steven M. Goodman[2,7], Cecilia Montauban[8,9], M. Corrie Schoeman[10], Beza Ramasindrazana[11], Carlos Ibáñez[12], Antonio Guillén-Servent[13], Javier Juste[12,14], Bruce D. Patterson[2]

[1]Department of Biology, Lund University, Lund 223 62, Sweden
[2]Negaunee Integrative Research Center, Field Museum of Natural History, Chicago, IL 60605, United States
[3]Department of Forestry and Wildlife Management, Maasai Mara University, Narok 20500, Kenya
[4]CIBIO-InBIO, Research Centre in Biodiversity and Genetic Resources, University of Porto, Vairão 4485-661, Portugal
[5]BiBio Research Group, Natural Sciences Museum of Granollers, Granollers 08402, Spain
[6]Mammalogy Section, Department of Zoology, National Museums of Kenya, Nairobi, Kenya
[7]Association Vahatra, Antananarivo BP 3972, Madagascar
[8]Department of Life Sciences, Imperial College London, Ascot SL5 7PY, United Kingdom
[9]Department of Life Sciences, Natural History Museum London, London SW7 5BD, United Kingdom
[10]School of Life Sciences, University of KwaZulu-Natal, Durban 4000, South Africa
[11]Institut Pasteur de Madagascar, Antananarivo BP 1274, Madagascar
[12]Estación Biológica de Doñana (CSIC), Seville 41092, Spain
[13]Instituto de Ecología A.C., Xalapa, Veracruz 91073, Mexico
[14]Epidemiology and Public Health, CIBERESP, Madrid 28029, Spain

*Corresponding authors. Daniela M. Rossoni, Department of Biology, Lund University, Kontaktvägen 10, Lund 223 62, Sweden.
E-mail: daniela.rossoni@gmail.com and Terrence C. Demos, Negaunee Integrative Research Center, Field Museum of Natural History, Chicago, IL 60605, USA.
E-mail: tdemos@fieldmuseum.org

Abstract

Accurate delimitation of species boundaries is crucial for uncovering evolutionary history and guiding conservation efforts in systematically complex groups. We evaluated species limits within the genus *Macronycteris*, large African roundleaf bats, using genetic, morphological, and bioacoustic data. Although mitochondrial DNA supported four reciprocally monophyletic species, nuclear introns revealed incomplete lineage sorting and limited genetic differentiation, suggesting recent diversification. Species delimitation analyses based on cytochrome *b* indicated up to eight putative lineages, whereas multi-locus analyses supported the five currently recognized species. Morphometric analyses of >300 specimens revealed significant interspecific differences in external and cranial traits, with *Macronycteris gigas* being markedly larger than congeners. Insular species were smaller than mainland forms, consistent with the island rule. Unlike most bats, all species exhibited strong male-biased sexual size dimorphism, but the extent of dimorphism did not follow Rensch's rule. Bioacoustic analyses differentiated species, with echolocation frequencies varying significantly across species and localities. Discriminant analyses of cranial and acoustic traits achieved high classification accuracy, reinforcing phenotypic distinctions among genetically similar taxa. Our results highlight a case of phenotypic and ecological divergence outpacing molecular differentiation in a recent bat radiation and provide a robust framework for species delimitation in *Macronycteris*, with implications for taxonomy, biogeography, and conservation.

Keywords cryptic diversity, insular dwarfism, integrative taxonomy, island rule, mito-nuclear discordance, phylogeography, Rensch's rule

Received: 1 October 2025. **Revised:** 1 June 2026. **Accepted:** 9 June 2026
© The Author(s) 2026. Published by Oxford University Press on behalf of The Linnean Society of London.
This is an Open Access article distributed under the terms of the Creative Commons Attribution License (https://creativecommons.org/licenses/by/4.0/), which permits unrestricted reuse, distribution, and reproduction in any medium, provided the original work is properly cited.

Downloaded from academic.oup.com/zoolinnean/article/207/4/zlag124/8770687 by guest on 27 August 2026

Introduction

Bats of the genus *Macronycteris* Gray, 1866 are the largest members of the Old World roundleaf bats (Family Hipposideridae) and are endemic to mainland sub-Saharan Africa, nearshore islands of the continent (i.e. Bioko, Quirimbas, and Zanzibar archipelago), and the oceanic islands of São Tomé and Madagascar (Monadjem 2019). Adult males of the two African species, the type species *Macronycteris gigas* (Wagner, 1845) and *Macronycteris vittata* (Peters, 1851), routinely exceed 100 g in body mass, and values of ≤180 g have been reported (Monadjem 2019). The species on Madagascar [*Macronycteris commersonii* (Geoffroy-Saint-Hilaire, 1813) and *Macronycteris cryptovalorona* (Goodman, Schoeman, Rakotoarivelo & Willows-Munro, 2016)] and São Tomé Island [*Macronycteris thomensis* (Bocage, 1891)] are smaller in measurements and body mass, but still large and robust bats. Insofar as is known, all members of the genus are strongly insectivorous; their size and powerful jaws and associated musculature permit them to feed on large, fortified beetles, in addition to softer-bodied arthropods (Vaughan 1977, Rakotoarivelo *et al.* 2009, Tuneu-Corral *et al.* 2025).

Five years after John Gray named this genus, Wilhelm Peters (1871) reduced *Macronycteris* to a subgenus within *Hipposideros*. By the time of Knud Andersen's revisions (Andersen 1905, 1906a, b), the use of *Macronycteris* even as a subgenus had ceased, and this group was recognized as the *H. commersoni* [sic: original spelling is *commersonii*] species group. A fuller taxonomic history of the family appears in the study by Hill (1963). That taxonomy persisted into the 21st century (Simmons 2005, Happold 2013), until Foley and colleagues (2015) showed that *Hipposideros* as traditionally composed was paraphyletic: the '*commersoni* group' diverged from other hipposiderids before the divergence of *Coelops* and *Hipposideros*. Subsequent work with fuller taxonomic sampling showed that *Macronycteris* and *Doryrhina* Peters, 1871 (formerly known as the *cyclops* group of *Hipposideros* and also endemic to Africa) formed a clade sister to the remaining hipposiderids (Foley *et al.* 2017, Patterson *et al.* 2020).

Genetic variation and population structure of African hipposiderids were recently surveyed by Patterson *et al.* (2020), whose study encompassed 453 individual bats from 192 localities. Well-supported mitochondrial clades were evident in *Macronycteris* (and in *Doryrhina* and *Hipposideros*), providing strong support for each of the four tested species of *Macronycteris* (*M. thomensis* was not included). Nevertheless, sequence variation in four unlinked nuclear introns raised questions concerning the evolutionary independence of these species. Reciprocal monophyly was lacking for three of the four species (it was evident only for the two known samples of *M. cryptovalorona*), and multi-locus lineage delimitation using the Bayesian Phylogenetics and Phylogeography (BPP) program (Yang 2015) on intron variation failed to support any of the *Macronycteris* species across the four prior schemes evaluated (Patterson *et al.* 2020). In contrast, the same introns and BPP analyses provided strong evidence of evolutionary independence among several putative cryptic species belonging to the *Hipposideros caffer* and *Hipposideros ruber* complexes. Previous studies have also documented phenotypic differentiation among *Macronycteris* species. Early field studies in East Africa reported consistent differences between *M. gigas* and *M. vittata* in external morphology, craniodental traits, and echolocation call frequencies (McWilliam 1982). Subsequent work on African hipposiderids has, likewise, recovered distinct genetic groupings corresponding to these taxa and highlighted the complex evolutionary relationships within the group (Monadjem *et al.* 2013). More recent integrative studies of Malagasy hipposiderids have further emphasized the importance of combining molecular and morphological data when evaluating species limits in this lineage (Rakotoarivelo *et al.* 2019). Together, these studies indicate that both phenotypic and genetic evidence is necessary to understand species boundaries and diversification patterns within *Macronycteris*.

Discordant patterns of variation in mitochondrial and nuclear DNA are not uncommon and have been reported in various groups of bats (Furman *et al.* 2014, Naidoo *et al.* 2016, Mao *et al.* 2017). Causes can include hybridization (either historical or ongoing), sex-biased dispersal, incomplete lineage sorting, demographic disparities, human introduction, or recency of divergence (Toews and Brelsford 2012, but see also Bonnet *et al.* 2017). In the present study, we aimed to assess the mito-nuclear discordance of *Macronycteris* species, both across Africa and regionally, with fine-grained information on patterns of variation in external morphology, cranial and dental morphology, echolocation calls, and their geographical distribution. We sought to determine whether *M. gigas* and *M. vittata* are independent evolutionary lineages, as suggested by their long taxonomic distinction and associated mitochondrial evidence, or whether the failure of species delimitation analyses to resolve these forms indicates conspecificity or more complicated evolutionary relationships (e.g. Morales and Carstens 2018). In addition, documentation of morphological and bioacoustic variation can provide additional criteria for diagnosing these species and understanding the factors underlying their diversification. Similar assessments were made of *M. commersonii* and *M. cryptovalorona* on Madagascar and *M. thomensis* on São Tomé Island, wherever possible using the same methodologies. Therefore, to clarify species limits and patterns of diversification within *Macronycteris*, we conducted an integrative assessment, combining mitochondrial and nuclear genetic data with cranial and external morphology and echolocation call structure across the geographical range of the genus. Our primary objective was to evaluate whether the currently recognized species represent independently evolving lineages when multiple sources of evidence are considered together. Specifically, we asked: (i) whether mitochondrial and nuclear genetic data provide concordant evidence for species boundaries; (ii) whether morphological and acoustic traits consistently differentiate taxa; and (iii) whether phenotypic variation across continental and insular populations provides additional insight into patterns of diversification within the genus. By integrating molecular, morphological, and bioacoustic evidence, we aim to provide a clearer taxonomic framework for *Macronycteris* and to gain a better understanding of the evolutionary processes underlying diversification in this group of large African roundleaf bats.

Downloaded from academic.oup.com/zoolinnean/article/207/4/zlag124/8770687 by guest on 27 August 2026

Materials and methods

DNA extraction, amplification, and sequencing

Genomic DNA was extracted from 36 tissue samples of *Macronycteris* using the QIAGEN DNeasy Blood and Tissue Kit (Qiagen, Hilden, Germany) following the manufacturer's protocols. An additional 76 *Macronycteris* sequences were downloaded from GenBank (Supplementary Appendix S1). Specimens were sequenced for mitochondrial cytochrome *b* (*Cytb*), using the primer pair LGL 765F and LGL 766R (Bickham *et al.* 1995, 2004), and seven unlinked autosomal nuclear introns (Igea *et al.* 2010), as follows: *SLC38A7* intron 8 (AAT), *ABHD11* intron 5 (ABHD11), *ACOX2* intron 3 (ACOX2), *ACPT* intron 4 (ACPT), *COPS7A* intron 4 (COPS7A), *ROGDI* intron 7 (ROGDI; Salicini *et al.* 2011), and *STAT5B* (Matthee *et al.* 2001). PCR products were purified using ExoSAP-IT (Thermo Scientific, Waltham, MA, USA). Sequencing was carried out in both directions at the Pritzker Laboratory for Molecular Systematics and Evolution at the Field Museum of Natural History (FMNH) and the Molecular Ecology Laboratory at Estación Biológica de Doñana Seville (EBD-CSIC). Chromatograms were edited and assembled in GENEIOUS PRIME v.2025.0.3 (Biomatters Ltd, Auckland, New Zealand). Sequences from each locus were aligned independently using the MUSCLE algorithm (Edgar 2004) with default settings in GENEIOUS. Protein-coding data from *Cytb* were translated to amino acids to determine codon positions and confirm the absence of premature stop codons, deletions, and insertions. Several gaps were incorporated in the nuclear intron alignments, but their positions were unambiguous. Newly generated sequence data have been deposited in GenBank under accession numbers (PX920326–PX920489) and are listed in Supplementary Appendix S1.

Phylogenetic inference

Maximum likelihood (ML) phylogenetic tree estimates of the *Cytb* and concatenated alignment of seven partitioned introns were inferred using the program IQ-TREE v.2.3.2 (Minh *et al.* 2020) on the CIPRES portal (Miller *et al.* 2010). The TESTNEW option was implemented using extended model selection that included the FreeRate model and was immediately followed by tree reconstruction using the best-fitting supported model. The UltraFast bootstrap algorithm (UFBS) and SH-aLRT (Shimodaira–Hasegawa-like approximate likelihood ratio test) supports were implemented using 1000 replicates. *Doryrhina camerunensis*, *Doryrhina cyclops*, *Hipposideros abae*, and *Cloeotis percivali* served as outgroups, based on the study by Patterson *et al.* (2020). Phylogenetic reconstruction under a Bayesian inference (BI) framework was inferred using the program MrBayes v.3.2.7 (Ronquist *et al.* 2012) for the same set of genes as the ML analyses, on the CIPRES portal. Two replicate MrBayes analyses were conducted using four Markov chains and 2×10^7 generations, with default heating values and sampling every 2000th generation, and with a burn-in of 25%. The HKY + Gamma substitution model was chosen and applied to each locus. Stationarity and mixing of MrBayes results were assessed in Tracer v.1.7.2 (Rambaut *et al.* 2018). Majority-rule consensus trees were constructed for each Bayesian analysis. PopART v.1.7 (Leigh and Bryant 2015) was used to construct a median-joining network of *Cytb* haplotypes within *Macronycteris*. Relative haplotype frequencies and relationships of haplotypes were depicted using pie charts in the network. Uncorrected sequence divergences (*p*-distances) within and between species were calculated for *Cytb* using MEGA v.12.0.8 (Kumar *et al.* 2024).

In our Bayesian time tree analyses, we estimated divergence times using fossil constraints to calibrate the molecular clock in *Macronycteris*. We assigned age priors on three nodes based on well-characterized fossils from the study by Amador *et al.* (2018) and references therein. A fossil calibration was placed on the time to most recent ancestor (TMRCA) of the monophyletic group *Cloeotis*, *Triaenops*, *Coelops*, *Aselliscus*, *Asellia*, *Hipposideros*, and *Rhinolophus* using a *Hipposideros* fossil dated to ~40 Mya, with a median age of 43.6 Mya, an SD of one, and an offset of 40 Mya. A second calibration was placed on the TMRCA of *Triaenops* and *Cloeotis* using a *Triaenops* fossil dated to >5.3 Mya with a median age of 10.9 Mya, an SD of one, and an offset of 5.44 Mya. A third calibration was placed on the TMRCA of the monophyletic group *Asellia*, *Hipposideros*, *Coelops*, and *Aselliscus* using an *Asellia* fossil dated to >20 Mya with a median age of 24 Mya, an SD of one, and an offset of 5.44 Mya. Uncertainty in these dates was accommodated by using a log normal prior probability distribution. We used BEAST v.2.7.7 (Bouckaert *et al.* 2019) to infer a time-calibrated tree. A fast lognormal relaxed-clock model was applied under a birth–death tree model, and a GTR + G substitution model was applied to the Cytb alignment. We used the Markov chain Monte Carlo chain on four replicates of 100 million generations and sampled trees every 10000 generations. Evidence for the convergence and stationarity of posterior model parameter distributions was assessed based on effective sample size values of >200 and examination of trace files in Tracer v.1.7. The burn-in was set at 10%, and separate runs were assembled using LOGCOMBINER v.2.7 and TreeAnnotator v.2.7.7 (Rambaut *et al.* 2018).

Species delimitation analyses

For all species delimitation analyses, we used the Mammal Diversity Database v.1.13 (2024) to define species limits for *Macronycteris*, which consists of five species: *M. commersonii*, *M. cryptovalorona*, *M. gigas*, *M. thomensis*, and *M. vittata*. DNA-based species delimitation was performed on the *Cytb* dataset using two single-locus approaches: the Poisson tree process model (PTP) and the single-threshold generalized mixed Yule coalescent model (GMYC). We designated each population from each gene-tree clade as a putative independent lineage, effectively putting a maximum on the number of lineages that could be delimited. The PTP was modelled using the program mPTP (Kapli *et al.* 2017). The mPTP is a single-locus coalescent-based method that uses a phylogenetic tree as input to identify the transition between species- and population-level divergence. The analysis was performed on the Exelixis Lab mPTP web server (https://mcmc-mptp.h-its.org/) using the ML tree generated in IQ-TREE v.2.3.2 as input. The program estimated a minimum branch length threshold in the ML trees and ignored branch lengths below it. Then

Downloaded from academic.oup.com/zoolinnean/article/207/4/zlag124/8770687 by guest on 27 August 2026

a single-threshold ML delimitation analysis was carried out using the Newick tree file, allowing for unique coalescent rates for each delimited species. We estimated support for the ML delimitation using Markov chain Monte Carlo runs of 1×10^7 generations, sampled every 1000 generations and with a burn-in of 20%. Starting delimitation was carried out using the null, random, and ML models in mPTP. The GMYC model (Fujisawa and Barraclough 2013) was also implemented on the Exelixis Lab GMYC web server. GMYC is a tree-based delimitation method that requires an ultrametric gene tree as input, with branching rates based on clock-like assumptions. The GMYC uses a likelihood approach to infer the timing of branching events on a phylogeny and searches for the most likely transition between Yule (interspecific) and a coalescent (intraspecific) branching structure (Fujisawa and Barraclough 2013). A *Cytb* ultrametric tree was inferred in BEAST v.2.7.7 (Bouckaert *et al.* 2019) on the CIPRES portal. The ultrametric tree *Cytb* dataset used a strict clock, Yule tree prior, and GTR + G substitution model, with all other priors set to defaults. Analyses were performed for 10^7 generations, with trees sampled every 1000 generations. BEAST log files were examined in Tracer to assess convergence and adequate posterior sampling (effective sample size > 200). A maximum clade credibility tree was estimated using median node heights in TreeAnnotator v.2.7.7 (Suchard *et al.* 2018) based on the sampled trees after discarding the first 10% as burn-in. The ultrametric tree inferred with BEAST was then used to perform the GMYC analysis. The Newick tree file from the BEAST analysis was run on the GMYC web server (https://species.h-its.org/gmyc/) using default settings.

We conducted joint independent lineage delimitation and species-tree estimation (analysis A11) using the program BPP v.4.8.43 (Yang 2015, Flouri *et al.* 2018) on the seven nuclear intron dataset for the five currently recognized *Macronycteris* species. The method uses the multispecies coalescent model to compare different models of species delimitation (Yang and Rannala 2010, Rannala and Yang 2013) and species phylogeny (Yang and Rannala 2014, Rannala and Yang 2017) in a Bayesian framework, accounting for incomplete lineage sorting attributable to ancestral polymorphism and gene tree/species tree discordance. A diffuse prior ($\alpha = 3$) was set for population size parameters (θ) and root divergence time (τ) following the recommendations by Flouri *et al.* (2020). Seven different prior combinations were implemented for the shape parameter setting (β) for both population size (θ), which varied from large (.01) to intermediate (.001) to small (.001), and root divergence time (τ), which varied from deep (.015) to intermediate (.0015) to shallow (.00015), based on the studies by Demos *et al.* (2018) and Marr *et al.* (2024), because BPP has been shown to be sensitive to effective population size and divergence time priors in determining the probability of delimitation (Yang and Rannala 2010). We tested the validity of our assignment of individuals to species using the guide-tree-free algorithm (A11) in BPP to avoid specifying a guide tree in advance. Two replicates were run for each of seven combinations of shape parameters (Supplementary Table S1). All BPP analyses were run for 10^5 generations, with a burn-in of 10^4 generations, and samples drawn every fifth generation.

External morphology

We analysed external morphological measurements from multiple individuals of *Macronycteris* species, including *M. commersonii* ($N = 14$), *M. cryptovalorona* ($N = 1$), *M. gigas* ($N = 111$), *M. thomensis* ($N = 33$), and *M. vittata* ($N = 107$). The dataset comprised total body length (TTL), body mass (WT), tail length (TL), ear length (EL), and forearm length (FA), along with information on sex and country of origin. The external measurements in millimetres (mm) were obtained from collectors' field catalogues or specimen labels. We chose to present these data because patterns in external measurements can be particularly useful for researchers in the field. However, we advise caution in their use, because there is considerable variation in how collectors take these measurements.

Prior to statistical analysis, data were cleaned to remove extreme outliers. Outliers were identified using the interquartile range method, and additional targeted filtering was performed based on species- and sex-specific thresholds. Measurements with missing values were excluded from relevant analyses. The assumption of normality was checked visually using histograms and boxplots, and homogeneity of variance was assessed using Levene's test. To compare variation in external morphological traits across species, we conducted one-way ANOVA tests followed by Tukey's honest significant difference (HSD) *post hoc* tests for pairwise comparisons to determine which species differed significantly from each other. Sex and country were also included as factors in the ANOVA models to account for sexual dimorphism and geographical variation.

To evaluate the effects of insularity and sexual dimorphism on body size in *M. gigas*, we performed two-way ANOVAs with interaction terms, using body mass (WT) and forearm length (FA) as response variables. We categorized individuals by geographical origin (Bioko Island vs. Continental Africa) and by sex (male or female), and included the interaction term (region × sex) to test whether the magnitude of regional differences varied between sexes. Only individuals with complete data for each trait and both factors were included in the analyses. All statistical analyses in this section and in the subsequent Materials and methods sections were carried out using R v.4.4.2 (R Core Team 2025). Data and R scripts are available in the GitHub repository (https://github.com/drossoni/Macronycteris).

Linear morphometric analysis

We analysed the cranial and dental morphology of 310 *Macronycteris* specimens housed in the Field Museum of Natural History, Chicago, IL (FMNH), the National Museum of Natural History, Washington, DC (USNM), the Estación Biológica de Doñana, Seville (EBD-CSIC), and the Université d'Antananarivo, Département de Biologie Animale, Antananarivo (UADBA), now the Mention Zoologie et Biodiversité Animale (Supplementary Appendix S1). Our analyses included the neotype of *M. commersonii* (FMNH 175972), and the holotype of

Downloaded from academic.oup.com/zoolinnean/article/207/4/zlag124/8770687 by guest on 27 August 2026

M. cryptovalorona (FMNH 175970). Morphometric variation was assessed based on 15 linear craniodental and mandibular measurements taken with digital callipers with .01 mm accuracy. Only adults, with fully erupted dentitions and fused cranial and phalangeal sutures, were measured for the following dimensions: GLS, greatest length of skull; CIL, condyloincisive length; CCL, condylocanine length; BB, braincase breadth; ZB, zygomatic breadth; PB, postorbital breadth; CC, palate width; MSTW, mastoid width; MPW, skull breadth; PL, palatal length; MTRL, maxillary toothrow length; MLTRL, maxillary molariform toothrow length; M2M2, width at M2; DENL, dentary length; and MANDL, mandibular toothrow length (Velazco and Gardner 2012). Linear distances are described in Supplementary Table S2. The measurement data were log-transformed and standardized to check the normality and potential outliers of each measurement. We used the multivariate imputation by chained equations (MICE) method to iteratively predict missing values in our analyses (see Supplementary 'Missing data analysis' section 2.1; Supplementary Tables S3–S6).

We established grouping hypotheses for the morphometric analyses based on the results of our previous molecular analyses (Patterson *et al.* 2020). The *a priori* grouping hypothesis consisted of five species, as follows (Mammal Diversity Database 2024): *M. commersonii* ($N = 41$), *M. cryptovalorona* ($N = 1$), *M. gigas* ($N = 109$), *M. thomensis* ($N = 33$), and *M. vittata* ($N = 126$). Individuals previously sequenced for *Cytb* and used in the present study are listed in Supplementary Appendix S1. To classify specimens lacking genetic information, we performed a linear discriminant analysis (LDA) using the genotyped individuals as training sets in the cross-validation tests and considered the LDA posterior probabilities in the classification decision. Additionally, we used the same approach to assign predicted sex information to individuals of *M. vittata* with unknown sex based on cranial trait variation.

The effects of sex and locality on cranial traits were assessed for each species using multivariate analysis of variance (MANOVA), with model selection based on Wilk's λ statistic ($P < .05$). Owing to significant effects of sex, locality, or their interaction (i.e. sex, sex + geography, or sex × geography), residuals from a general linear model (GLM) were used in subsequent analyses. In addition to using GLM residuals, an alternative approach for correcting categorical effects involves fitting a linear model to remove factor effects while preserving the global mean, then adding the global mean back to the residuals to maintain the overall scaling of the data. Both approaches performed well with our data. We performed a principal component analysis to explore which morphological variables contributed the most to the variation of each axis and to identify which variables were most informative to discriminate species in the subsequent discriminant function analysis. A discriminant function analysis was applied on each group to test whether the morphometric variables could discriminate individuals according to the *a priori* morphological hypothesis based on molecular results. To assess the classification performance of the model, we used leave-one-out cross-validation, wherein each specimen was classified based on discriminant functions derived from all remaining observations. Overall and species-specific classification accuracies were calculated by comparing predicted group memberships with observed classifications. Pairwise Mahalanobis distances between species centroids were also calculated to quantify multivariate morphological divergence. We first extracted group means from the LDA model and computed the pooled within-group covariance matrix using the raw cranial measurements. Mahalanobis distances were calculated as the square root of the generalized squared distance between species means, using the inverse of the pooled covariance matrix. The species *M. cryptovalorona* was excluded from this analysis owing to its representation by a single specimen, which precluded estimation of within-group variance.

After establishing the categories of all specimens, we estimated and tabulated descriptive statistics separately by sex, including the mean, range (minimum and maximum) and SE. To investigate differences among species, we conducted a one-way ANOVA for each trait, assessing whether species means were significantly different. If a significant effect was found ($P < .05$), we performed Tukey's *post hoc* HSD tests to determine pairwise differences between species.

Echolocation call recordings and analysis

In Kenya, vocalizations of *Macronycteris* individuals were recorded using a Pettersson D1000X handheld ultrasound detector (Pettersson Elektronik AB, Uppsala, Sweden; 384 kHz sampling rate, 16-bit resolution). On Madagascar, calls of individual bats were recorded with an Avisoft Ultrasound 116Hb Bat Detector (Avisoft Bioacoustics, Berlin, Germany; 300 kHz sampling rate, 16 bits, mono, with a threshold of 16) connected to an HP Pavillion 6210 notebook (Hewlett Packard Development Company, Palo Alto, CA, USA). In Equatorial Guinea and Ghana, echolocation calls were recorded using Wildlife Acoustics Echo Meter Touch 2 Pro Android (Wildlife Acoustics, Inc., Maynard, MA, USA; Firmware Version: App 2.8.14; 384 kHz sampling rate, 16-bit resolution) on Galaxy and Samsung smartphones. In São Tomé, echolocation calls were recorded with a Pettersson D980 ultrasound detector (Pettersson Elektronik AB, Uppsala, Sweden; 350 kHz sampling rate, 8-bit resolution), from which ×10 time-expanded analog output was recorded onto metal -XR Sony cassette tapes using a Sony WM-D6C cassette recorder. Tape recordings were re-digitized in the laboratory with a sonagraph (DSP-5500; Kay Elemetrics Corp.) at a sampling rate of 40 kHz (attaining a 400 kHz effective sampling rate over the original recordings). The detectors used in this study are digital recorders with high sampling frequencies that offer full-spectrum recording capability and capture the full bandwidth of the call (Moir *et al.* 2013). All bats were held in the hand ~30 cm away from the microphone while recording. Bats were handheld to avoid the Doppler-shift compensation associated with flight; the 'resting frequency' of stationary individuals varies very little within a sequence (Fenton *et al.* 2012, Hiryu *et al.* 2016). Consequently, calls of handheld bats are best suited for frequency comparisons between individuals or populations.

Downloaded from academic.oup.com/zoolinnean/article/207/4/zlag124/8770687 by guest on 27 August 2026

Macronycteris uses a perch-hunting foraging behaviour, with a low-frequency form of echolocation, dominated by low-repetition-rate calls (Vaughan 1977, Webala *et al.* 2019). A customized 512-point fast Fourier transform was performed for sound analysis, together with a Hanning window for both spectrograms and power spectrum. Echolocation calls were characterized by measuring peak frequency or frequency with maximum energy (FME), maximum frequency (StartF), minimum frequency (EndF), duration (Dur), and bandwidth (BW) using KALEIDOSCOPE v.3.1.4b (Wildlife Acoustics, USA), or the Kay DSP-5500 sonagraph in the case of the São Tomé recordings, and following Jung *et al.* (2014). The mean of 10 calls with the best signal-to-noise ratios was calculated for each individual. Researchers recorded vocalizations of 221 *Macronycteris* individuals (65 *M. commersonii*, 60 *M. gigas*, 57 *M. thomensis*, and 39 *M. vittata*; Supplementary Appendix S1); recordings of *M. cryptovalorona* are not available. Prior to analysis, records with missing values for any of the involved variables were removed.

Initially, we investigated intraspecific variation in call parameters for each species independently, testing whether factors such as sex and locality influenced the vocalization variables. We also tested the relationship between FME and forearm length (FA) whenever these continuous variables were available in the dataset. To assess whether sex and locality influence the call parameters, a two-way ANOVA was conducted. The model included sex, locality, and their interaction as independent variables, as follows:

$$Y = \beta_o + \beta_1 \text{Sex} + \beta_2 \text{Locality} + \beta_3 \left(\text{Sex} \times \text{Locality}\right) + \varepsilon,$$

where Y represents each call parameter, β_o is the intercept, and ε represents residual error.

We fitted a multiple linear regression model to determine whether FME is influenced by FA (a proxy for relative body size) while considering the factors sex and locality, as follows:

$$\begin{aligned}\text{FME} = \beta_o + \beta_1 \text{FA} + \beta_2 \text{Sex} + \beta_3 \text{Locality} + \beta_4 \left(\text{FA} \times \text{Sex}\right) \\ + \beta_5 \left(\text{FA} \times \text{Locality}\right) + \beta_6 \left(\text{FA} \times \text{Sex} \times \text{Locality}\right) + \varepsilon.\end{aligned}$$

The preceding models were adapted according to the available data for each species.

We also investigated interspecific variation in call parameters for all species together, correcting for the influence of categorical variables whenever necessary. Given that FME was the only call parameter available for *M. thomensis*, we considered that variable only when the four species were analysed together. To assess differences in call structure among species, we performed a one-way ANOVA for each acoustic parameter across the four species. In cases where the assumptions of normality or homogeneity of variances were not met, Kruskal–Wallis tests were used as non-parametric alternatives. Given that *M. commersonii*, *M. gigas*, and *M. vittata* had complete datasets for all call parameters, we conducted independent *t*-tests (Welch's *t*-test) to examine differences between these three species. To evaluate the ability of acoustic traits to differentiate species, we applied an LDA. The model was trained using FME, StartF, EndF, Dur, and BW as predictor variables, with species identity (*M. gigas* and *M. vittata*) as the classification label. Data were split into training (70%) and testing (30%) sets, and model performance was assessed using classification accuracy, precision, recall, and F1-score.

We considered males and females together in the description of basic statistics after determining that males and females in the dataset did not differ in their call frequencies ($P > .05$). For each species and call parameter, we then calculated basic descriptive statistics, including means, range, and SDs. Finally, we used one-way ANOVAs to test whether bats from each species had equal call frequencies among species, followed by Tukey's *post hoc* test to determine which groups differed significantly from others.

Results

Genetics

Species of *Macronycteris* are only weakly differentiated in terms of mitochondrial DNA sequences (Table 1). *Cytb* distances between species range from 1.3% (between *M. thomensis* and *M. gigas*) to 3.1% (between *M. thomensis* and *M. cryptovalorona*). There is nearly as much variation among the 30 used *M. commersonii* sequences as that distinguishing *M. thomensis* from *M. gigas*.

The ML *Cytb* tree (Fig. 1) recovers four *Macronycteris* species as monophyletic, but the weakly supported *thomensis* clade is nested within *gigas* (Table 1). Poor support for short backbone internodes in the tree fails to resolve relationships among species, although the monophyly of *Macronycteris* is strongly supported, as is its sisterhood with *Doryrhina*. The BI tree (Supplementary Fig. S1) has a different topology but also supports the same four species as monophyletic; again, *M. thomensis* renders *M. gigas* paraphyletic. As in the ML tree, backbone nodes were poorly

Table 1 Genetic distances between nominal species of *Macronycteris*.

	M. commersonii	*M. cryptovalorona*	*M. gigas*	*M. thomensis*	*M. vittata*
M. commersonii	**.012**				
M. cryptovalorona	.028	**.003**			
M. gigas	.024	.027	**.009**		
M. thomensis	.027	.031	.013	**.003**	
M. vittata	.026	.029	.024	.029	**.006**

The number of base differences per site is averaged among 103 nucleotide sequences over 1140 base positions of cytochrome *b*. Entries shown in bold on the diagonal measure intraspecific variation in our samples.

Downloaded from academic.oup.com/zoolinnean/article/207/4/zlag124/8770687 by guest on 27 August 2026

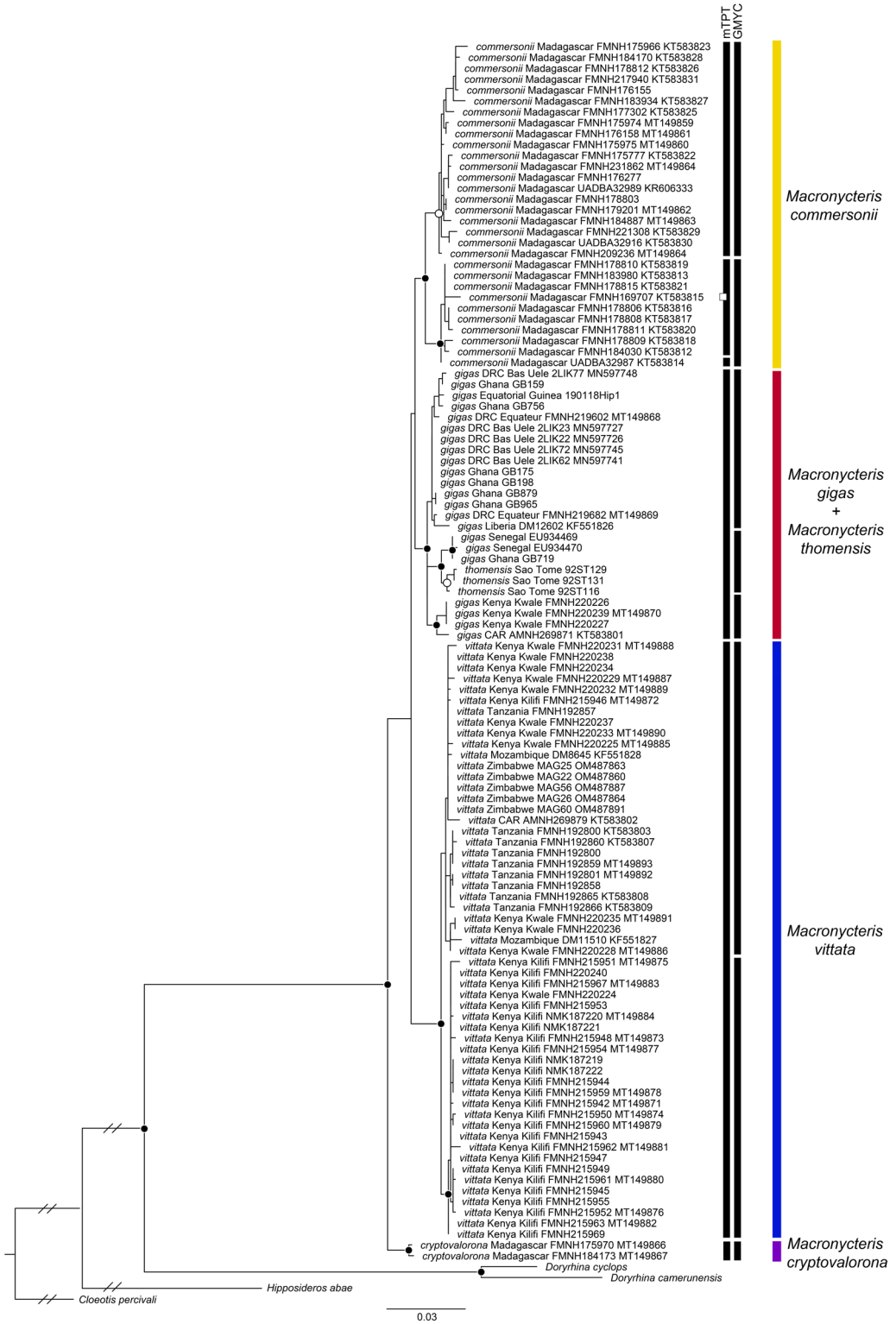


Figure 1 Maximum likelihood phylogeny of *Macronycteris* specimens based on mitochondrial cytochrome *b* sequences. The phylogeny was inferred in IQ-TREE. Black circles on nodes denote bootstrap (BS) values of ≥95%, and white circles denote BS values between 90% and 94%. Support values for most minor clades are not shown.

supported, and relationships among species were unresolved, except for *M. thomensis*, which was strongly supported as nested within *M. gigas*.

A haplotype substitution network (Fig. 2) identifies the geographical component of *Cytb* substitutions. Few substitutions distinguish the five species. Although most haplotypes were restricted to a single country, a common haplotype of *M. vittata* is found in specimens from Kenya, Tanzania, Mozambique, and Zimbabwe, and a common haplotype of *M. gigas* extends from Ghana through Equatorial Guinea to the

Downloaded from academic.oup.com/zoolinnean/article/207/4/zlag124/8770687 by guest on 27 August 2026

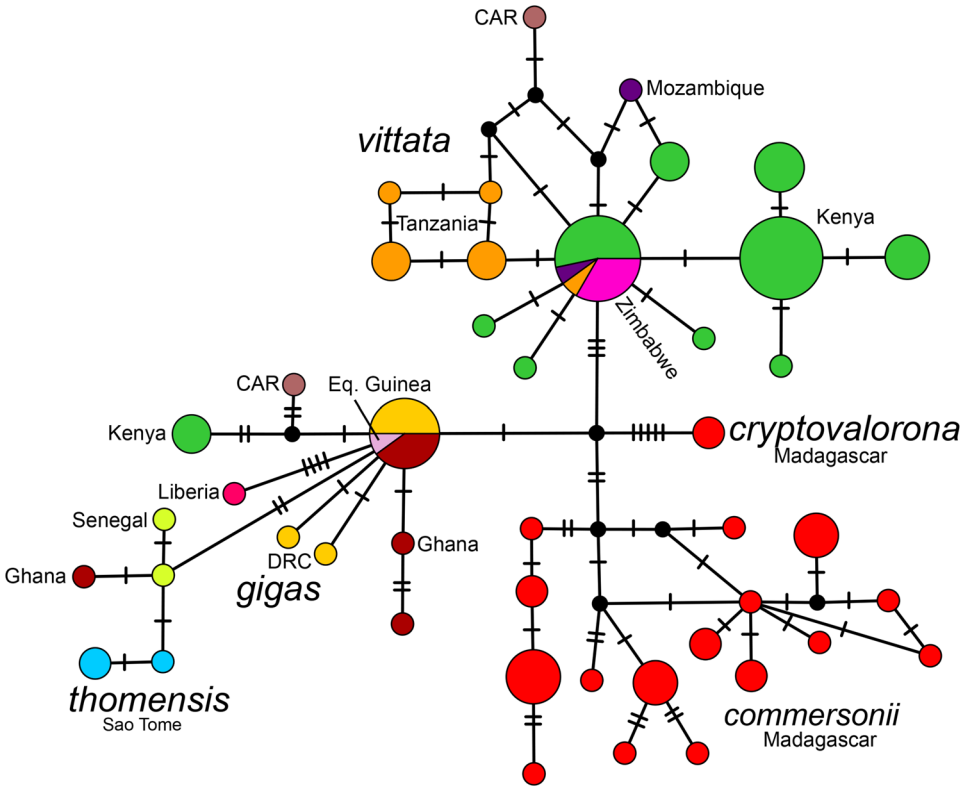


Figure 2 Median-joining network of cytochrome *b* haplotypes of five *Macronycteris* species inferred in PopART v.1.7. Coloured circles represent different sampled haplotypes by country, and black circles represent inferred missing or unsampled states. Hatch marks denote mutational steps between haplotypes. Abbreviations: CAR, Central African Republic; DRC, Democratic Republic of Congo.

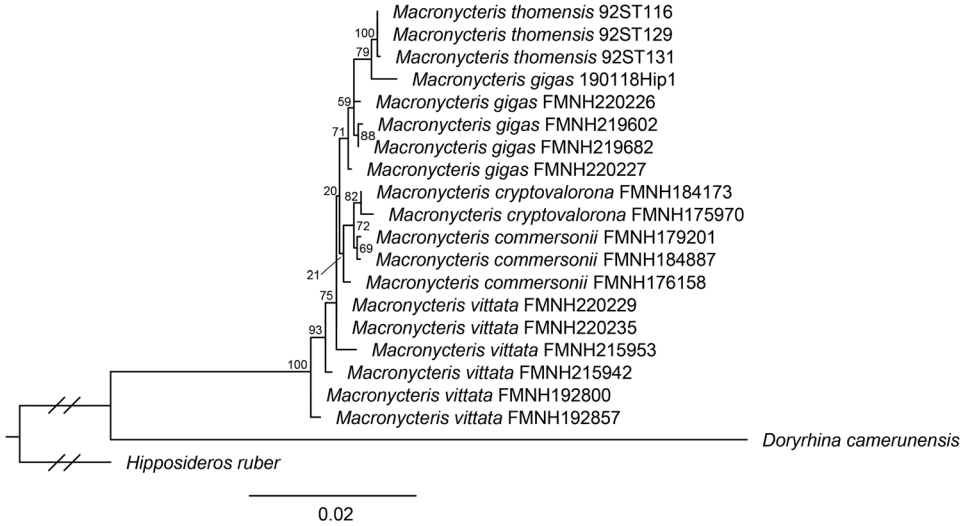


Figure 3 Maximum likelihood gene tree of *Macronycteris* species based on a concatenated alignment of seven independent nuclear intron loci. The phylogeny was inferred in IQ-TREE. Numbers adjacent to nodes indicate bootstrap support.

Democratic Republic of Congo (DRC). For *M. gigas*, *M. vittata*, and *M. commersonii*, intraspecific variation among haplotypes exceeds the substitutions distinguishing their neighbours.

A concatenated alignment of seven nuclear introns challenges the reciprocal monophyly of *Macronycteris* taxa, as shown in the ML tree (Fig. 3) and the BI tree (Supplementary Fig. S2). Only *M. thomensis* and *M. cryptovalorona* are recovered as monophyletic, although support for *M. cryptovalorona* was low (UFBS = 82). The two Malagasy species are recovered as sisters, but without much support; *M. cryptovalorona* renders *M. commersonii* paraphyletic, just as *M. thomensis* renders *M. gigas* paraphyletic. Strikingly, all of these species appear to have shared common ancestry more recently than *M. vittata* populations. It would appear that the pairs *M. gigas* + *M. thomensis* and *M. commersonii* + *M. cryptovalorona* were each derived from ancestral populations of *M. vittata*.

Downloaded from academic.oup.com/zoolinnean/article/207/4/zlag124/8770687 by guest on 27 August 2026

The slight genetic differentiation of *Macronycteris* species in mitochondrial sequences and their lack of reciprocal monophyly in the nuclear intron tree suggest that their differentiation has been recent. A time tree analysis (see Supplementary Fig. S3) suggests that the differentiation of crown *Macronycteris* species has taken place over the last 3.97 Myr.

Species delimitation analysis implementing the single-threshold model in mPTP estimated seven lineages as putative species in the *Cytb* dataset with support values of .99: *M. cryptovalorona*, *M. vittata*, *M. gigas*, and four lineages within *M. commersonii* (Fig. 1). *Macronycteris thomensis*, nested within *M. gigas* in the *Cytb* ML tree, was not supported as distinct. The GMYC *Cytb* analysis estimated eight lineages as putative species: *M. cryptovalorona*, two lineages in *M. vittata*, three lineages in *M. gigas*, and two lineages in *M. commersonii*; *M. thomensis* was not supported as distinct (Fig. 1). In both single-locus analyses, only *M. commersonii* was inferred to be a single putative species congruent with current taxonomy. Results from a series of replicated BPP analyses using the seven-intron dataset differed in posterior probability (PP) of the number of putative species delimited with strong support (PP $\geq$ .95). Prior schemes 3–7 supported the five species taxonomy with PP $\geq$ .98 (Supplementary Table S1), with every species in these prior combinations having PP $\geq$ .95. In contrast, prior schemes 1 and 2, which had a mean θ of .001, failed to support any species number, including lumping all five recognized *Macronycteris* species.

External morphology

Across all species, ANOVAs revealed significant effects of species, sex, and country for every external trait examined (all $P < .001$). Tukey's HSD tests showed that *M. gigas* differed significantly from other species in nearly all traits. *Macronycteris gigas* had significantly greater values for body mass (WT), forearm length (FA), tail length (TL), and ear length (EL) compared with *M. commersonii* and *M. vittata*. For total body length (TTL), only *M. gigas* differed significantly from *M. commersonii*. Ear length followed a similar pattern, with *M. gigas* displaying significantly longer ears than *M. commersonii* and *M. vittata*. Descriptive statistics for external morphology of *Macronycteris* species and sex are presented in Table 2.

Boxplots depicting the distribution of each external measurement across species, along with ANOVA results and HSD tests, are provided in Supplementary Figs S4–S9 and Supplementary Tables S7–S21. Importantly, we recognize the influence of measurement variability introduced by an unbalanced dataset and various collectors taking standardized measurements in a slightly different way; this limits the usefulness of multivariate analyses.

The Mann–Whitney *U*-tests performed to compare island and continental populations revealed that body mass (WT; mean, 95.0 vs. 116.1 g; $U = 394.0$, $P = .0034$) and forearm length (FA; mean, 103.2 vs. 107.3 mm; $U = 95.0$, $P = .0039$) were both significantly reduced in insular specimens, consistent with patterns of island dwarfism (Fig. 4; Supplementary Table S19).

The two-way ANOVA results showed that both region (Bioko Island vs. Continental Africa) and sex had significant effects on body mass and forearm length in *M. gigas* (WT: region, $F = 16.70$, $P = .0001$; sex, $F = 37.14$, $P = .0001$; FA: region, $F = 14.15$, $P = .0006$; sex, $F = 13.95$, $P = .0007$; Supplementary Tables S20 and S21). However, the interaction between region and sex was not significant for either trait (WT: $F = .07$, $P = .79$; FA: $F = 0.10$, $P = .76$; Supplementary Tables S20 and S21), indicating that the effects of region and sex on body size were additive and not dependent on each other. These results provide evidence for insular dwarfism in *M. gigas*, with individuals from Bioko Island being significantly smaller than those from Continental Africa in both body mass and forearm length (Fig. 5). Importantly, the lack of significant interaction between region and sex suggests that the difference in size between Bioko Island and continental populations is consistent across sexes. Both males and females from Bioko Island exhibit reduced body size relative to their continental counterparts, and sexual size dimorphism is maintained regardless of geographical origin. These patterns support the hypothesis that insular populations of *M. gigas* have undergone parallel reductions in body size attributable to ecological or evolutionary constraints associated with island life.

Table 2 Descriptive statistics for external morphological traits in *Macronycteris* species.

Species	Sex (*N*)	TTL	WT	TL	EL	FA
M. commersonii	F (7)	130 (120–140)	46.4 (30–64)	29.3 (25–35)	28 (26–30)	85.3 (76–93)
M. commersonii	M (7)	137.7 (125–156)	56.2 (33–69)	26 (25–28)	24.3 (20–28)	91.3 (85–95)
M. cryptovalorona[a]	F (1)	123 (123–123)	55 (55–55)			80 (80–80)
M. gigas	F (48)	149.1 (137–169)	97.5 (62–131)	36.7 (22–48)	33.4 (29–36)	102.3 (96.4–110)
M. gigas	M (63)	164.2 (142–180)	124.4 (71–188)	41.7 (25–52)	32.9 (24–40)	106.6 (99.1–114)
M. thomensis	F (14)		47.3 (29.5–65)			81.7 (78.3–84.6)
M. thomensis	M (19)		58.1 (39.5–85)			86.1 (81–89)
M. vittata	F (51)	130.1 (113–150)	64.9 (46–110)	28 (20–39)	29 (23–32)	90.5 (87.5–98)
M. vittata	M (52)	141.8 (105–180)	109.4 (85–170)	34 (22–45)	30.1 (20–35)	102.1 (90–118)

Data are separated by females (F) and males (M) followed by sample size (*N*). The mean value is presented, followed by minimum and maximum values in parentheses. Abbreviations: EL, ear length; FA, forearm length; TL, tail length; TTL, total body length; WT, body mass. [a]For *M. cryptovalorona*, the only available material is of females.

Downloaded from academic.oup.com/zoolinnean/article/207/4/zlag124/8770687 by guest on 27 August 2026

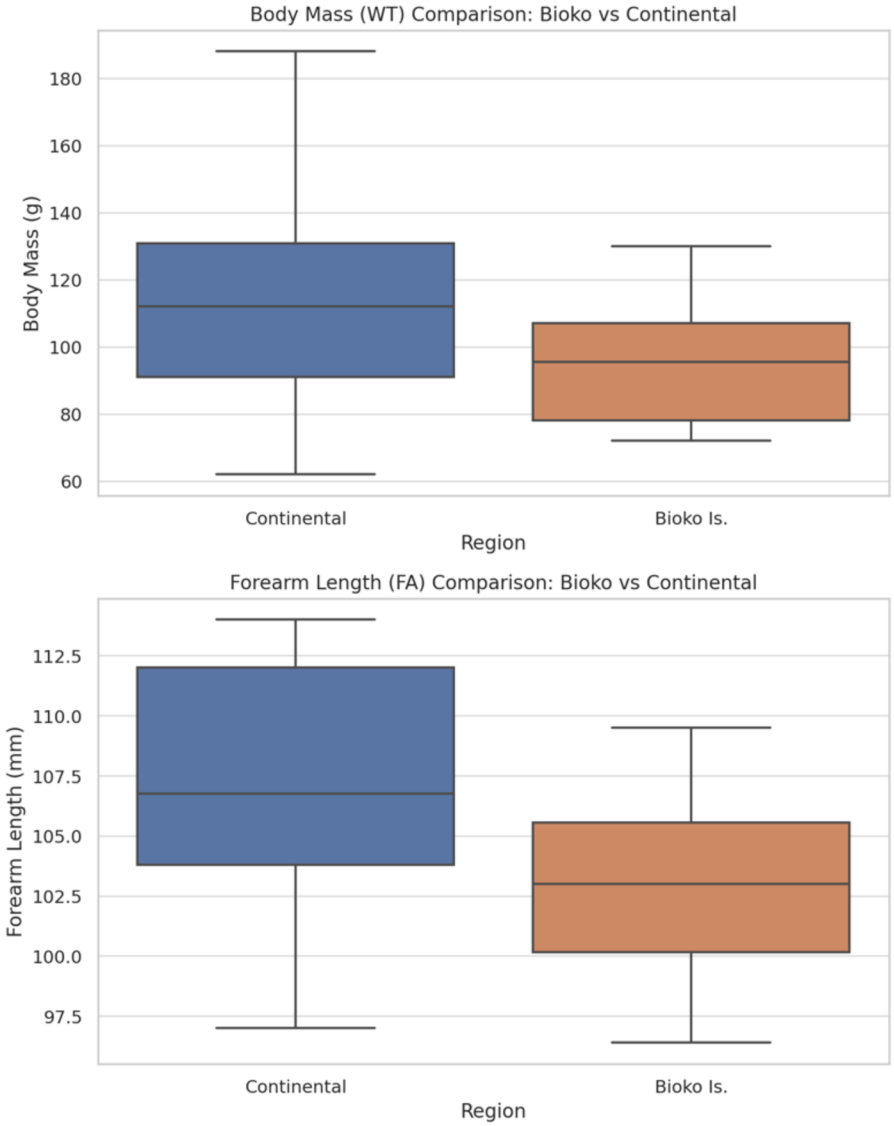


Figure 4 Comparisons of body mass (WT) and forearm length (FA) of *Macronycteris gigas* from Bioko Island vs. Continental Region.

Craniodental morphometrics

Intraspecific variation

The effects of categorical variables on cranial traits of *Macronycteris* species are summarized in Supplementary Table S22. The MANOVA assessing the additive effects of sex and geography on *M. gigas* cranial traits revealed a statistically significant effect of sex on cranial morphology (Wilks' $\lambda = .219$, $F_{15,76} = 18.1$, $P < .001$), indicating strong sexual dimorphism in this species. Locality also had a highly significant effect (Wilks' $\lambda = .020$, $F_{75,368.24} = 6.2$, $P < .001$), suggesting substantial geographical variation in cranial traits among populations. However, the interaction between sex and locality was not significant (Wilks' $\lambda = .567$, $F_{45,193.88} = .91$, $P = .641$), indicating that the influence of sex on cranial traits remains consistent across geographical regions. Consequently, we used residuals from the additive model (excluding the interaction term) for subsequent analyses.

The additive effects of sex and locality on the dependent variables were also examined in *M. vittata*. Our results revealed a highly significant effect of sex (Wilks' $\lambda = .35879$, $F_{15,105} = 12.51$, $P < .001$) and geography (Wilks' $\lambda = .40857$, $F_{30,210} = 3.95$, $P = .001$), indicating that males and females differ significantly in their multivariate cranial traits and that these traits also exhibit substantial geographical variation. The significant main effects of sex and geography suggest that both factors contribute independently to cranial morphological variation. The relatively low Wilks' λ values (closer to zero) for both predictors indicate that a substantial proportion of variance in the dependent variables is explained by sex and geography. Notably, the effect of sex on cranial morphology appears particularly strong in *M. vittata*, as reflected by the large *F*-statistic and highly significant *P*-value.

The results of the MANOVA indicated a statistically significant effect of sex on cranial morphology in *M. commersonii* (Wilks' $\lambda = .178$, $F_{15,25} = 7.7$, $P < .001$) and *M. thomensis*

Downloaded from academic.oup.com/zoolinnean/article/207/4/zlag124/8770687 by guest on 27 August 2026

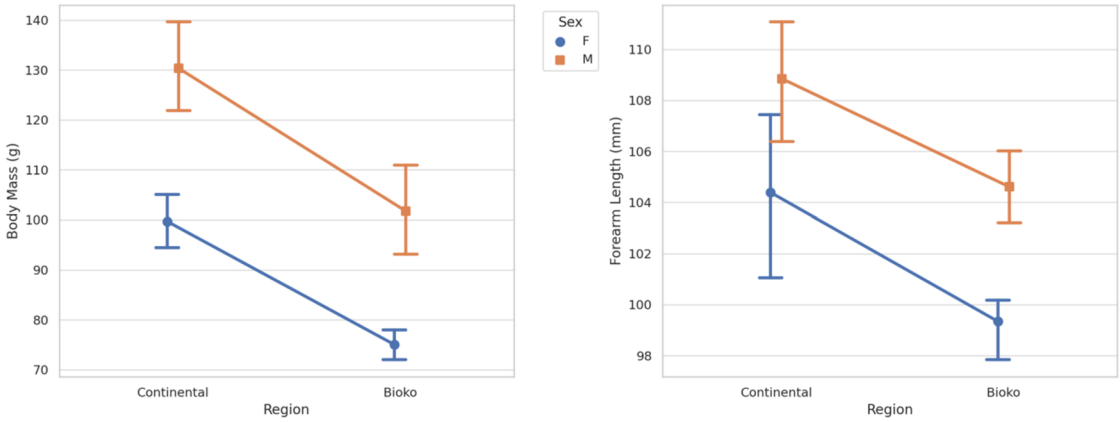


Figure 5 Interaction plots showing the effects of region (Bioko Island vs. Continental Africa) and sex on body mass (WT; left) and forearm length (FA; right) in *Macronycteris gigas*. Points represent group means with 95% confidence intervals. Both body mass and forearm length show significant effects of region and sex, but no significant interaction, indicating consistent insular dwarfism across sexes.

(Wilks' $\lambda = .159$, $F_{15,17} = 6.0$, $P < .001$), suggesting strong sexual dimorphism in cranial traits for both species. The low Wilks' λ values (.178 and .159, respectively) indicate that sex accounts for a large proportion of variance in cranial traits, with only ~18% and ~16% of the variance remaining unexplained by this categorical variable. Additionally, the *F*-statistics (7.7 and 6.0, respectively) further support the substantial differences between sexes across multiple cranial traits. Statistical tests could not be performed for *M. cryptovalorona* owing to a sample size of only one individual; thus, only descriptive statistics are reported for this species.

Interspecific variation

Given that the MANOVA results revealed significant sexual dimorphism, we tabulated the variable means, ranges, and SEs separately for each species and sex (Tables 3 and 4). Descriptive statistics for 138 females revealed variation in cranial traits across species, with *M. gigas* generally displaying the largest trait values (Table 3). The ANOVA results indicated significant differences among species for all traits analysed ($P < .05$; Supplementary Table S23). Tukey's *post hoc* HSD tests identified multiple significant pairwise differences in cranial traits between species (Supplementary Table S24). For instance, *M. gigas* exhibited significantly larger values compared with all other species across multiple traits. Likewise, *M. vittata* and *M. thomensis* showed significant differences in several measurements when compared with *M. commersonii* and *M. cryptovalorona*. These results suggest strong morphological differentiation among the five species considering all females in our sample, with some species clustering more closely in trait distributions than others.

Descriptive statistics for 172 male specimens revealed notable variation in cranial traits across the four species (*M. commersonii*, *M. gigas*, *M. thomensis*, and *M. vittata*; Table 4). Similar to the female analyses described above, *M. gigas* exhibited the largest cranial trait values, whereas *M. commersonii* had the smallest. ANOVA results demonstrated statistically significant differences among species for all traits analysed ($P < .05$; Supplementary Table S24), indicating substantial interspecific variation in the cranial morphology of males. Tukey's *post hoc* HSD tests further identified multiple significant pairwise differences in cranial traits (Supplementary Table S25). *Macronycteris gigas* consistently displayed significantly larger values than all other species across multiple traits, reinforcing its morphological distinctions. Additionally, *M. vittata* and *M. thomensis* differed significantly from *M. commersonii* in several cranial measurements, suggesting species-specific morphological patterns. These results highlight strong morphological differentiation among the four species in our male samples, with some species clustering more closely in trait distributions than others. Considering both male and female results (Tables 3 and 4), our findings reinforce the role of cranial traits in species differentiation and suggest potential ecological or evolutionary drivers underlying these patterns.

The principal component analysis and additional exploratory analyses of interspecific variation in male and female samples are reported in the Supplementary material (Supplementary section 4.1; Supplementary Figs S10–S12; Supplementary Tables S26–S29). The discriminant function analysis performed to test species-level morphological differentiation in cranial traits among *Macronycteris* is presented in Fig. 6 and Supplementary Fig. S13. The analysis yielded four linear discriminant (LD) functions, of which the first three explained most of the interspecific variation (LD1 = 73.8%, LD2 = 21.7%, and LD3 = 4.3%). Species centroids in the discriminant space were well separated, with *M. gigas* positioned furthest along the positive end of the reversed LD1 axis, consistent with its status as the largest species in the genus (Fig. 6; Supplementary Fig. S13). In contrast, *M. commersonii* and *M. cryptovalorona* occupied the negative end of this axis, reflecting their smaller cranial size. *Macronycteris vittata* and *M. thomensis* showed intermediate positions, with *M. vittata* notably separating along LD2 (Fig. 6). The variables contributing most strongly to LD1 were GLS, CCL, BB, and CC, which together captured variation associated with overall cranial size and shape.

Cross-validation and posterior group means further supported clear morphological distinction among species. Leave-one-out cross-validation yielded an overall classification accuracy of 96.4%, with individual species accuracy

Downloaded from academic.oup.com/zoolinnean/article/207/4/zlag124/8770687 by guest on 27 August 2026

Table 3 Descriptive statistics of craniodental and mandibular measurements (in millimetres) for *Macronycteris* females.

Measurement	Statistics	*M. commersonii*	*M. cryptovalorona*	*M. gigas*	*M. thomensis*	*M. vittata*
	Number of females	24	1	45	14	54
GLS	Mean	28.83	28.85	37	31.01	32.17
	Min–Max	27.35–31.51		34.83–39.06	30.46–31.71	30.27–38.25
	SE	.2		.13	.09	.2
CIL	Mean	25.49	24.3	32.86	26.92	28.97
	Min–Max	23.78–27.81		30.44–34.52	26.18–28.07	27.17–34.51
	SE	.2		.13	.11	.18
CCL	Mean	25.27	24.26	32.37	26.23	28.47
	Min–Max	23.9–27.37		30.5–34.92	25.58–26.94	26.67–33.28
	SE	.19		.12	.12	.17
BB	Mean	10.96	10.64	13.16	11.55	11.86
	Min–Max	10.04–11.7		11.87–13.88	11.16–12.09	10.74–13.71
	SE	.09		.07	.08	.08
ZB	Mean	15.23	14.8	20.46	16.76	17.53
	Min–Max	14.51–16.23		19.06–22.11	16.09–17.8	16.14–20.8
	SE	.09		.1	.12	.12
PB	Mean	3.1	2.89	3.76	3.28	3.73
	Min–Max	2.76–3.4		3.22–4.53	3.03–3.67	3.1–4.33
	SE	.03		.04	.05	.03
CC	Mean	6.93	6.73	9.98	6.73	8.8
	Min–Max	6.11–8.29		7.67–11.3	6.11–7.39	8.06–10.57
	SE	.12		.14	.1	.07
MSTW	Mean	11.69	11.75	14.58	12.38	12.78
	Min–Max	11.13–12.38		13.59–15.71	12.04–12.88	11.54–14.92
	SE	.08		.06	.06	.08
MPW	Mean	13.24	12.73	16.44	14.11	14.44
	Min–Max	12.52–14.13		15.43–17.64	13.8–14.44	13.12–16.85
	SE	.1		.06	.05	.11
PL	Mean	9.04	8.98	11.98	10.37	10.69
	Min–Max	8.33–9.65		11.42–13.22	10.05–10.6	9.98–11.98
	SE	.09		.07	.04	.06
MTRL	Mean	10.21	9.68	13.53	11.11	11.45
	Min–Max	9.54–11.15		12.63–14.68	10.84–11.4	10.42–14.01
	SE	.09		.05	.05	.09
MLTRL	Mean	7.74	7.44	10.1	8.21	8.54
	Min–Max	7.28–8.38		9.35–10.59	7.8–8.54	7.84–10.72
	SE	.06		.04	.05	.08
M2M2	Mean	10.21	9.69	13.35	10.55	11.28
	Min–Max	9.6–10.96		12.39–14.24	9.98–11.25	10.27–13.19
	SE	.07		.05	.08	.09
DENL	Mean	19.69	18.91	25.75	20.81	22.35
	Min–Max	18.61–21.62		24.22–27.12	20.22–21.92	20.75–26.17
	SE	.17		.09	.13	.14
MANDL	Mean	11.39	10.93	15.35	12.48	12.94
	Min–Max	10.57–12.36		14.44–15.98	12.14–13.04	11.91–16.19
	SE	.1		.05	.08	.12

ranging from 93% (*M. vittata*) to 95.1% (*M. commersonii*) to 100% (*M. gigas* and *M. thomensis*). Pairwise Mahalanobis distances between group centroids in discriminant space reflected strong morphological differentiation among *Macronycteris* species (Supplementary Table S30). The greatest distance was observed between *M. gigas* and *M. commersonii* ($D = 8.9$), consistent with their extreme positions along the primary discriminant axis. The smallest distance occurred

Downloaded from academic.oup.com/zoolinnean/article/207/4/zlag124/8770687 by guest on 27 August 2026

Table 4 Descriptive statistics of craniodental and mandibular measurements (in millimetres) for *Macronycteris* males.

Measurement	Statistics	*M. commersonii*	*M. gigas*	*M. thomensis*	*M. vittata*
	Number of males	17	64	19	72
GLS	Mean	31.09	39.39	32.83	35.84
	Min–Max	28.44–32.6	35.87–42.14	30.04–34.42	30.87–42.28
	SE	.28	.19	.29	.25
CIL	Mean	27.3	34.38	27.89	31.66
	Min–Max	25.62–29.02	30.94–36	26.49–28.69	27.73–37.88
	SE	.23	.14	.13	.19
CCL	Mean	27.23	33.79	27.55	31.18
	Min–Max	25.57–28.44	30.82–35.35	26.55–28.12	27.4–37.21
	SE	.19	.13	.09	.2
BB	Mean	11.54	13.72	11.92	12.59
	Min–Max	10.74–12.25	12.49–14.83	11.06–12.51	10.73–13.81
	SE	.1	.06	.09	.07
ZB	Mean	16.68	22.26	18.29	19.6
	Min–Max	15.07–17.73	20.14–24.07	16.83–19.9	16.22–24.18
	SE	.19	.13	.22	.17
PB	Mean	3.19	3.84	3.18	3.65
	Min–Max	2.79–3.53	3.18–4.53	2.87–3.58	2.97–4.06
	SE	.05	.04	.04	.03
CC	Mean	7.88	10.43	7.54	9.74
	Min–Max	7.11–8.79	7.96–11.84	6.49–8.28	7.96–12.16
	SE	.13	.14	.11	.1
MSTW	Mean	12.6	15.33	13.04	13.9
	Min–Max	11.79–13.17	14.18–16.8	12.5–13.61	11.8–15.26
	SE	.08	.06	.08	.06
MPW	Mean	14.45	17.98	15.52	16.54
	Min–Max	13.28–15.58	15.4–19.91	13.83–16.87	13.45–20.08
	SE	.18	.12	.24	.16
PL	Mean	9.59	12.8	10.86	11.58
	Min–Max	8.59–10.47	11.42–14.11	10.2–11.44	10.2–14.5
	SE	.13	.07	.09	.09
MTRL	Mean	10.72	13.91	11.53	12.25
	Min–Max	10.01–11.14	12.71–14.91	11.11–12.02	10.25–14.4
	SE	.07	.05	.06	.08
MLTRL	Mean	8.06	10.17	8.4	9.02
	Min–Max	7.57–9.23	9.32–10.87	8.01–8.78	8.14–10.24
	SE	.1	.05	.05	.05
M2M2	Mean	10.63	13.72	10.92	12.04
	Min–Max	9.96–11.53	12.72–14.99	10.51–11.3	10.42–14.02
	SE	.1	.06	.05	.08
DENL	Mean	21.24	27.07	22.2	24.44
	Min–Max	20.04–21.98	24.54–28.47	21.01–23.03	21.46–28.6
	SE	.14	.11	.14	.15
MANDL	Mean	12.37	16.03	13.14	14.09
	Min–Max	11.55–13.15	14.54–16.89	12.7–13.8	12.37–16.3
	SE	.1	.06	.07	.08

Downloaded from academic.oup.com/zoolinnean/article/207/4/zlag124/8770687 by guest on 27 August 2026

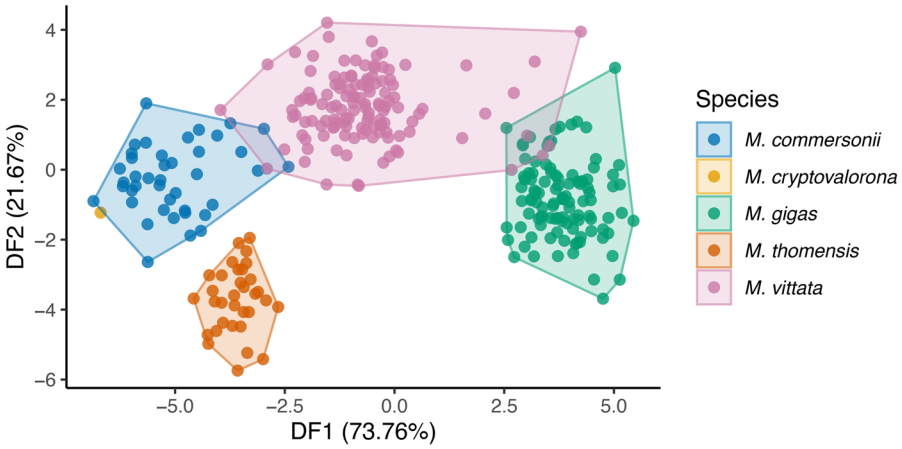


Figure 6 Linear discriminant function axes (DF1 and DF2) of craniodental and mandibular variables performed for all *Macronycteris* samples.

between *M. commersonii* and *M. vittata* ($D = 5.2$), although all pairwise distances exceeded $D = 4.7$, indicating distinct cranial morphologies (Supplementary Table S30).

Echolocation calls

Intraspecific variation

The two-way ANOVA revealed that locality significantly influenced all acoustic parameters ($P < .05$) in *M. commersonii*, whereas sex had no significant effect on any variable (Supplementary Fig. S14). Additionally, a significant sex × locality interaction was observed for FME ($P = .0087$), StartF ($P = .0083$), and EndF ($P = .0390$), suggesting that variation in acoustic frequency differs between localities but not consistently between sexes. No significant interaction was detected for call duration ($P = .64$) or bandwidth ($P = .24$), and the effect of sex on bandwidth could not be evaluated owing to insufficient data. *Post hoc* tests confirmed significant pairwise differences in echolocation call parameters between various localities, indicating geographical variation in call structure (Supplementary Tables S31 and S32).

The results from multiple regression analysis testing the influence of body size (forearm length, FA), sex, and geography on the FME in *M. commersonii* showed that the model was highly significant ($F_{7,51} = 34.56$, $P < .001$) and explained a substantial proportion of the variation in FME ($R^2 = .826$), indicating that these factors contribute meaningfully to differences in call frequency. In our analyses, FA emerged as a significant predictor of FME ($P = .001$), with a negative relationship between FA and FME ($\beta = -.3869$). This suggests that larger individuals produce echolocation calls with lower FME (Fig. 7), highlighting a potential size-related variation in call structure (to visualize the relationships between FA and FME by locality, see Supplementary Fig. S15). In contrast, sex did not have a significant effect on FME ($P = .552$), indicating that males and females produce calls with similar frequencies when accounting for forearm length and locality.

In *M. gigas*, the two-way ANOVA revealed that geography significantly influenced FME ($P < .001$), EndF ($P < .001$), duration ($P = .018$), and bandwidth ($P = .01$), whereas sex had no significant effect on any call parameter for this species (Supplementary Table S33; Supplementary Fig. S16). Our results also showed a significant interaction between sex and geography for FME ($P = .003$), suggesting that the effect of sex on FME varies across countries (as seen in Supplementary Fig. S16). The multiple regression analysis demonstrated that FA did not significantly predict FME ($P = .901$) in *M. gigas* (Fig. 7). Additionally, sex and geography were not significant predictors of FME in this model (all *P*-values >.2), and no significant interaction effects were observed between FA, sex, and geography, indicating a lack of relationship between these variables.

Only the variable FME was available for analysis in *M. thomensis*. The two-way ANOVA showed that FME varies significantly by geographical location (Mendes da Silva and Santa Ana; $P < .001$), thus confirming that geographical variation is a key factor in acoustic differences in *M. thomensis*. The other hipposiderid found on the island of Sao Tomé (*Hipposideros ruber*) also shows high geographical variation in CF values. In that case, the variation is determined by the variable environmental conditions (particularly humidity) found around the colony (Guillén-Servent *et al.* 1999). Sex alone had no significant effect on FME ($P = .774$), again suggesting no acoustic differences between males and females in this species. Moreover, the interaction between sex and geography was not significant ($P = .530$), meaning that the effect of geography on FME is consistent across sexes (Supplementary Fig. S17). The multiple regression demonstrated that forearm length did not significantly predict FME ($P = .276$) in *M. thomensis* (Fig. 7). Additionally, sex and geography were not significant predictors of FME in this model (all *P*-values >.3), and no significant interaction effects were observed between FA, sex, and locality, indicating a lack of relationship between these variables.

The two-way ANOVA results for *M. vittata* indicated that sex and geography had no significant effects on any of the five vocalization traits (all *P*-values >.05; Supplementary Table S34). There was no evidence of an interaction between sex and geography, suggesting that these factors do not strongly influence acoustic call parameters in *M. vittata* (Supplementary Fig. S18; Supplementary Table S34). The multiple regression model revealed that FA had a significant negative effect on FME ($P = .045$), indicating that individuals with longer forearms produced lower minimum frequencies

Downloaded from academic.oup.com/zoolinnean/article/207/4/zlag124/8770687 by guest on 27 August 2026

Table 5 Descriptive statistics for call frequencies (in kilohertz) and duration (in milliseconds) of *Macronycteris* species.

Parameter	Statistics	*M. commersonii*	*M. gigas*	*M. vittata*	*M. thomensis*
FME	Mean	70.91	53.66	68.04	68.20
	Min–Max	63.3–78.9	51.15–54.96	65.08–69.91	64.14–69.51
	SD	4.91	.82	1.57	.88
StartF	Mean	72.3	54.50	68.95	
	Min–Max	64.8–80.2	52.70–58.77	66.02–71.09	
	SD	4.94	.90	1.56	
EndF	Mean	68.47	47.05	59.21	
	Min–Max	51.2–77	40.05–53.42	53.57–66.23	
	SD	5.27	2.76	3.02	
Duration	Mean	11.67	12.60	14.46	
	Min–Max	7.5–17	6.59–22.70	7.0–21.0	
	SD	2.17	2.92	3.56	
Bandwidth	Mean	3.73	6.52	9.73	
	Min–Max	2.5–8.7	2.22–11.24	1.60–13.62	
	SD	1.51	2.44	3.02	

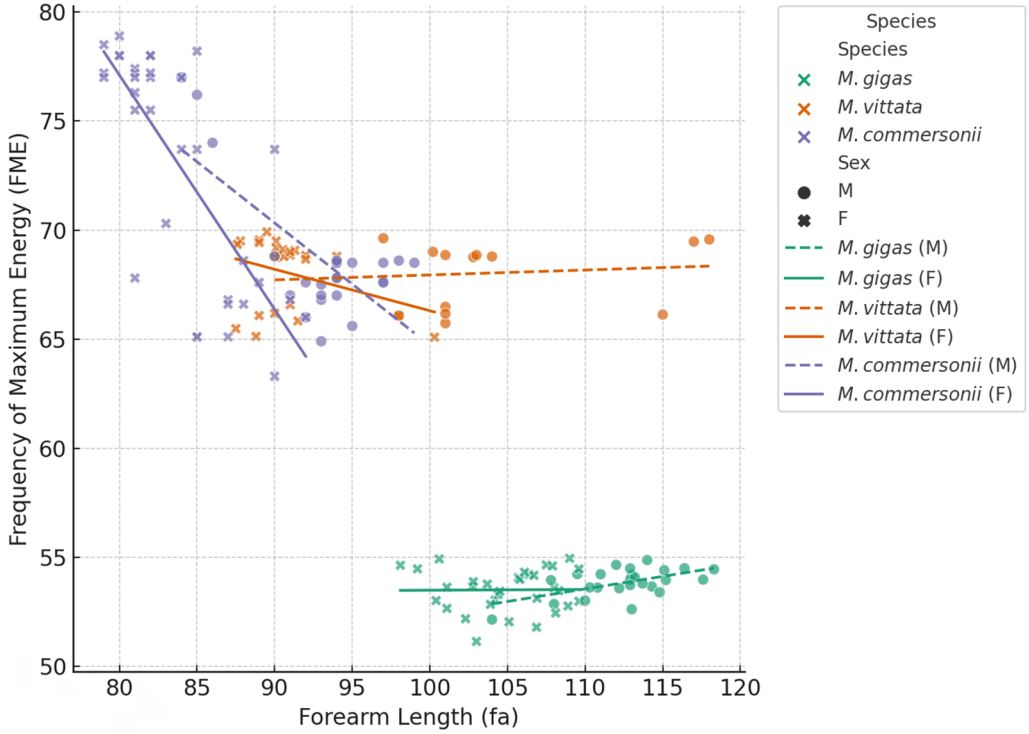


Figure 7 Scatterplot and regression lines of frequency of maximum energy (FME) and forearm length (fa) for each *Macronycteris* species and sex.

(Fig. 7). However, neither sex nor locality had a significant effect on FME, and interaction terms were non-significant. Additionally, the overall model had low predictive power (R^2 = .197, adjusted R^2 = .010), suggesting that additional factors influence FME beyond those included in the model.

Interspecific variation

Descriptive statistics of acoustic parameters for 221 *Macronycteris* individuals across the four species (*M. commersonii*, *M. gigas*, *M. thomensis*, and *M. vittata*) are presented in Table 5.

The one-way ANOVA showed a significant effect of species on FME ($F_{3,217}$ = 459.72, P < .001). Further *post hoc* comparisons demonstrated that the FME of *M. commersonii* was significantly higher than that of *M. gigas* (mean difference = 17.26 kHz, P < .001), *M. thomensis* (mean difference = 2.71 kHz, P < .001), and *M. vittata* (mean difference = 2.87 kHz, P < .001). Additionally, *M. gigas* exhibited significantly lower FME compared with both *M. thomensis* (mean difference = −14.54 kHz, P < .001) and *M. vittata* (mean difference = −14.38 kHz, P < .001). However, there was no significant difference in FME between *M. thomensis*

Downloaded from academic.oup.com/zoolinnean/article/207/4/zlag124/8770687 by guest on 27 August 2026

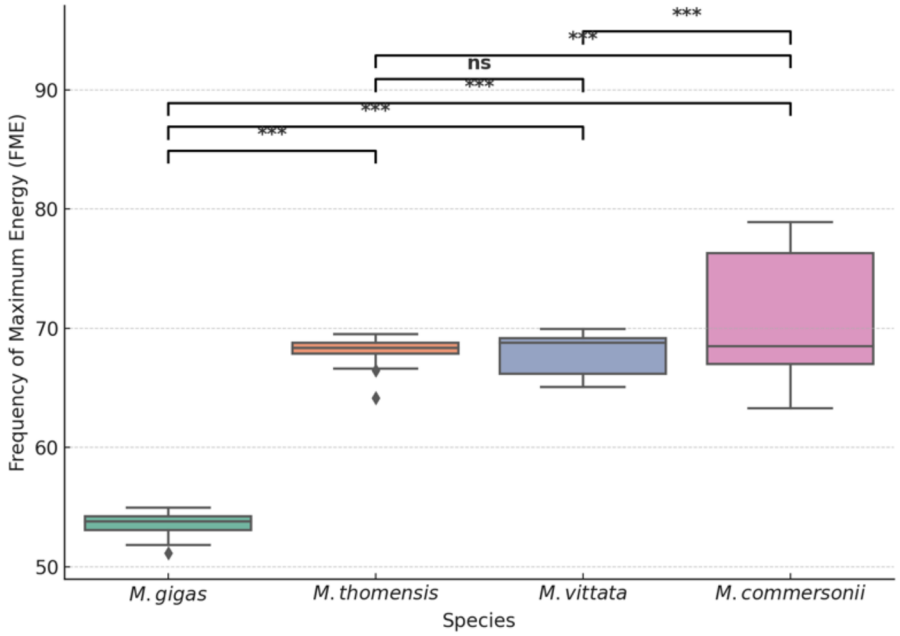


Figure 8 Boxplot illustrating differences in the frequency of maximum energy (FME; in kilohertz) between *Macronycteris* species with pairwise statistical significance annotations from Welch's *t*-tests: ***$P < .001$; ns, not statistically significant.

and *M. vittata* ($P = .993$), showing that these two species use similar echolocation frequencies (Fig. 8). These findings indicate substantial species-specific variation in FME, with *M. commersonii* having the highest values and *M. gigas* the lowest (Fig. 8).

The one-way ANOVA for the other parameters besides FME showed that all these variables exhibited significant differences among *M. gigas*, *M. vittata*, and *M. commersonii* ($P < .001$; *M. thomensis* was not included in these analysis, because data for these other echolocation variables were missing for the species), suggesting strong interspecific variation in call structure among these three species (Fig. 9; Table 5). For StartF and EndF, *M. gigas* exhibited significantly lower values compared with *M. vittata* and *M. commersonii*. Call duration varied notably among species, with *M. vittata* producing significantly longer calls than *M. commersonii* and *M. gigas* ($P < .001$). Likewise, bandwidth differed across species, with *M. commersonii* exhibiting the widest bandwidth, highlighting further divergence in echolocation call structure.

The LDA model, used to investigate whether FME alone could classify the four species accurately, achieved an overall classification accuracy of 62.1%, indicating that FME provides moderate discriminatory power in distinguishing species (Supplementary Table S35). The confusion matrix revealed that certain species were more distinguishable than others, with some misclassifications occurring, particularly between *M. thomensis* and *M. commersonii*. These results suggest that although FME is informative for species differentiation, additional acoustic parameters might be needed to improve classification accuracy. Following this result, we used an LDA model to assess whether multiple acoustic predictor variables (FME, StartF, EndF, duration, and bandwidth) could classify species accurately. Our model, trained and tested on *M. gigas*, *M. vittata*, and *M. commersonii* (excluding *M. thomensis* owing to missing data), achieved an overall classification accuracy of 97.9%, indicating high discriminatory power and minimal misclassifications.

The ANCOVA results demonstrated that forearm length significantly influenced FME in *M. gigas*, *M. vittata*, and *M. commersonii*, although the strength and direction of this relationship varied among species (see Fig. 7). For instance, in *M. gigas* and *M. vittata*, neither FA nor sex had a significant effect on FME ($P > .05$), indicating little or no correlation. In *M. commersonii*, FA showed a significant negative correlation with FME ($P < .001$), with larger males exhibiting lower FME than smaller females ($P = .049$). The interaction term (FA × sex) was also significant ($P = .034$), indicating that the relationship between forearm length and FME has a different slope between sexes in this species (Fig. 7).

Discussion

Our study of *Macronycteris* across its Afrotropical-Malagasy distribution highlights how phenotypic and ecological divergence can outpace genetic differentiation in recent radiations. Different data partitions offer distinctly different views on the diversification of the genus. We discuss each line of evidence in sequence.

Genetics and phylogenetics

The tempo of divergence among Macronycteris species

The five currently recognized species of *Macronycteris* are strongly supported as a monophyletic group, sister to the Afrotropical endemic genus *Doryrhina* (Foley *et al.* 2017, Patterson *et al.* 2020). Despite the Eocene divergence of the clade from *Doryrhina* (cf. Kumar *et al.* 2017), the extant species appear to be recent with respect to their differentiation. In terms of *Cytb* distances (Table 1), none of the

Downloaded from academic.oup.com/zoolinnean/article/207/4/zlag124/8770687 by guest on 27 August 2026

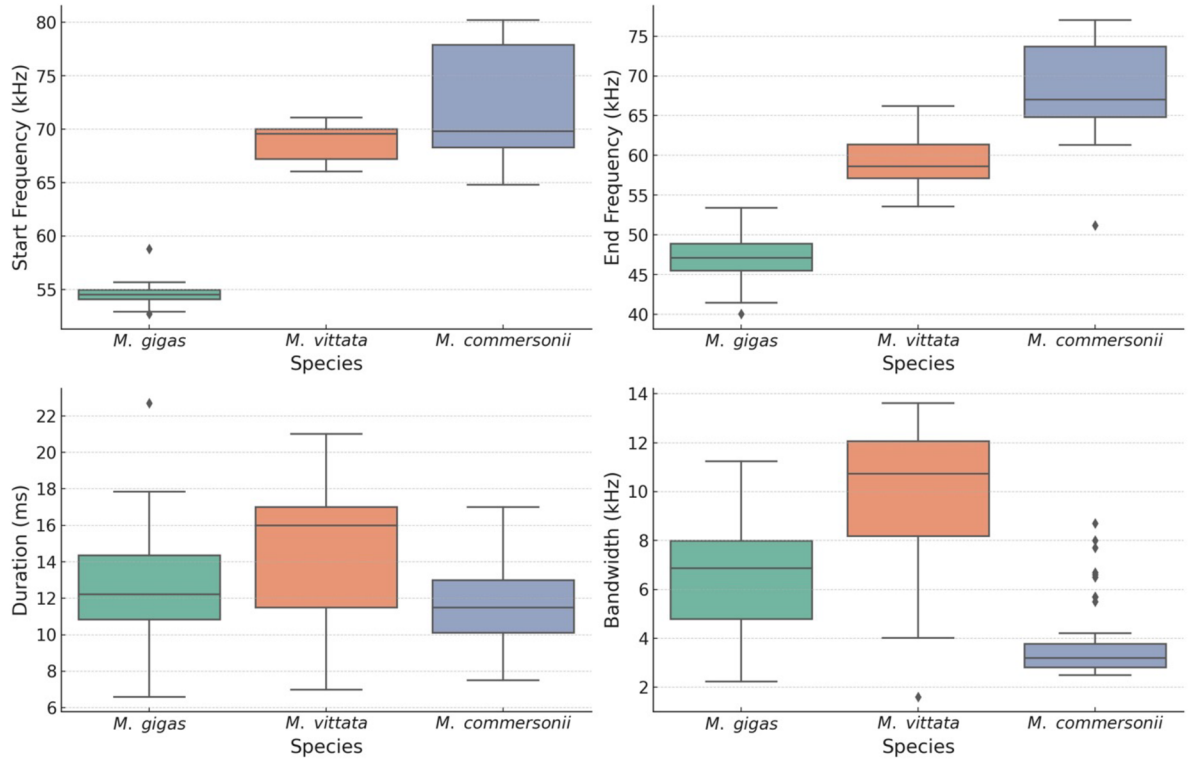


Figure 9 Boxplots illustrating the differences of multiple echolocations call parameters for *Macronycteris* species differentiation.

five species differs from others by >3.1%. This represents modest genetic differentiation among mammalian congeners. In a survey of polytypic rodents and bats, Bradley and Baker (2001) found that *Cytb* distances of <2% were indicative of infraspecific differences, distances of >11% corresponded to specific differences, and intermediate values required additional information to clarify their taxonomic rank, although there are cases of exceptionally low *Cytb* specific differences between recognized bat species (e.g. Puechmaille *et al.* 2014). The haplotype substitution network (Fig. 2) graphically illustrates the weak genetic differentiation among *Macronycteris* species, with more substitutions separating different haplotypes within *M. commersonii*, *M. gigas*, and *M. vittata* than those separating these species from each other.

Despite the slight differentiation of *Macronycteris* species in terms of *Cytb*, four of the five species were supported as monophyletic in both the ML and BI analyses (Fig. 1; Supplementary Fig. S1). However, *M. thomensis* was consistently recovered as nested within populations of *M. gigas*. There was little support for the deeper nodes in the *Cytb* tree, leaving relationships of species (beyond *M. thomensis* + *M. gigas*) unresolved. The short genetic distances, nested relationship, and poor backbone support are consistent with a recent diversification of these bats and/or post-divergence introgression. Recent ancestry or gene flow is also indicated by the variation of nuclear intron sequences. The ML and BI trees (Fig. 3; Supplementary Fig. S2) both showed *M. thomensis* as strongly nested within *M. gigas* and *M. cryptovalorona* as sister to *M. commersonii* (ML analysis) or rendering *M. commersonii* paraphyletic (BI analysis). However, only *M. thomensis* and *M. cryptovalorona* were recovered as monophyletic groups. As with mitochondrial sequences, the backbone nodes lack strong support. In both trees, *M. vittata* individuals appear as the most basal lineages.

Several factors could explain the genetic similarity despite the clear phenotypic divergence of these bats, including the conflicting signals between mitochondrial and nuclear gene sequences. We consider three primary explanations.

Incomplete lineage sorting and hybridization

The short genetic distances in mitochondrial DNA and the reciprocal monophyly of most species align with a recent divergence combined with rapid evolution of the mitochondrial genome and putative female philopatry in *Macronycteris* (e.g. Vaughan 1977, Arnold and Wilkinson 2015). However, the lack of reciprocal monophyly in the intron trees is probably a reflection of incomplete lineage sorting, whereby descendent lineages variably retain ancestral polymorphisms (Degnan and Rosenberg 2009, Lopes *et al.* 2021, Tomasco *et al.* 2022). This pattern is expected in species that have diverged recently, where ancestral alleles might persist owing to large effective population sizes or limited post-speciation drift (Maddison and Knowles 2006). Additionally, the presence of genetic nesting and conflicting nuclear–mitochondrial signals might suggest historical or ongoing hybridization. In this case, hybridization could obscure genetic differentiation by facilitating gene flow between species, leading to a homogenization of mitochondrial and nuclear markers (Mallet 2005, Petit and Excoffier 2009). Further investigations using genome-wide sequencing (e.g. restriction site-associated DNA sequencing

Downloaded from academic.oup.com/zoolinnean/article/207/4/zlag124/8770687 by guest on 27 August 2026

or whole-genome data) could help to resolve whether *Macronycteris* species are subject to post-divergence introgression, particularly in those species in widespread sympatry (i.e. *M. gigas* and *M. vittata*).

Selection-driven divergence and ecological differentiation

Despite their overall genetic uniformity, the different *Macronycteris* species exhibit diagnosable differences in phenotypic traits, particularly in craniodental morphology and vocalizations. This suggests that ecological and behavioural selection pressures might have driven phenotypic divergence in the absence of deep genetic differentiation (see Nosil *et al.* 2009, Funk *et al.* 2012). In many bat species, echolocation call structure is shaped by habitat acoustics and foraging strategy, which could lead to divergence in call frequencies and bandwidth even when neutral genetic variation remains similar (Guillén-Servent *et al.* 1999, Schnitzler and Kalko 2001, Jones and Holderied 2007, Denzinger and Schnitzler 2013). Likewise, differences in skull morphology might reflect dietary specialization and differences in prey availability, further reinforcing ecological divergence despite their retained ancestral polymorphism (Freeman 1981, Dumont 2007, Santana and Cheung 2016). Additionally, studies in phyllostomid bats have demonstrated that cranial covariation and morphological differentiation are influenced by multiple adaptive peaks related to feeding ecology and roosting behaviour, further supporting the role of selection in driving morphological divergence (Rossoni *et al.* 2017, 2019). These patterns align with theoretical models of phenotypic divergence preceding genetic divergence, whereby selection on key adaptive traits (e.g. vocalizations or foraging strategy) drives speciation independently of genome-wide divergence (Nosil *et al.* 2009).

The geographical distribution and habitat preferences of the different *Macronycteris* lineages suggest a potential role of ecological selection in species differentiation. The continental species have distributions centred on moist forests (*M. gigas*) and drier savannah woodlands (*M. vittata*; Happold 2013, Patterson *et al.* 2020, Monadjem *et al.* 2024). The taxonomy of *M. gigas* warrants further scrutiny. The type locality in southern Angola (Benguela) is not associated with continuous lowland rainforest, raising questions about whether the type specimen corresponds to the forest-associated populations currently identified as *M. gigas* (Monadjem 2019). It is therefore possible that the taxon as presently defined encompasses lineages historically referred to as *M. gambiensis* or *M. niangarae*. A comprehensive integrative revision will be necessary to clarify species limits and nomenclature within this complex that would include incorporation of historical DNA from synonymized type specimens.

In contrast, *M. commersonii* occurs in a wide range of forest ecosystems with different bioclimatic characteristics, from moist to dry deciduous and spiny forests (Goodman and Ramasindrazana 2013), spanning >1400 km along a north–south gradient. Such ecological breadth might account for the greater variability observed in its morphological, acoustic, and genetic parameters relative to other members of the genus. Habitat structure can influence echolocation call design because sound propagation and prey detection depend on environmental conditions (Schnitzler and Kalko 2001). Higher-frequency calls attenuate more rapidly in humid air, reducing detection distance and the range over which echoes can be perceived (Hartley 1992; Monadjem 2019). Conversely, lower-frequency calls travel farther but provide lower resolution for detecting small targets. In contrast, higher-frequency calls can generate echoes from smaller objects, such as flying insects, and allow finer resolution of moving targets (Pye 1960). Thus, higher frequencies may be favoured in open drier environments, where reduced attenuation allows effective detection and classification of small prey over longer distances. Conversely, lower frequencies may provide advantages in forested habitats, where higher humidity increases attenuation of high frequencies and reduces the range of prey detection and classification. In practice, the evolution of echolocation frequency is likely to reflect the combined effects of atmospheric attenuation, prey detection, habitat structure, and body size rather than a single environmental gradient. Consistent with this view, some hipposiderid and rhinolophid bats living in relatively dry habitats have been reported to use higher FME relative to body size than populations inhabiting wetter environments (Guillén-Servent *et al.* 1999; Heller and Helversen 1989), suggesting that these patterns are shaped by multiple interacting ecological factors. Additionally, habitats of different structure and composition are likely to host different prey communities, which could drive variation in skull morphology and reinforce ecological divergence. To test these hypotheses, comparative ecological, behavioural, and morphometric analyses are needed. These might include: (i) acoustic analysis to compare echolocation parameters across habitat types and evaluate the influence of atmospheric humidity and vegetation density on call structure (Heller and Helversen 1989, Guillén-Servent *et al.* 1999, Jacobs *et al.* 2017); (ii) metabarcoding or stable isotype analysis to assess dietary variation between species and test whether trophic niche differentiation aligns with morphological divergence (for an example of the latter with cricetid rodents, see Missagia *et al.* 2019) or possible evidence for migratory populations tracking food resources; (iii) geometric morphometric studies to quantify cranial shape variation in relationship to habitat type and prey preferences (e.g. Budinski *et al.* 2015; Ospina-Garcés *et al.* 2016); and (iv) genomic scans for selection and identification of candidate genes associated with sensory adaptations and dietary preferences (e.g. Gutiérrez-Guerrero *et al.* 2020). These approaches offer a comprehensive framework for evaluating the role of ecological selection in shaping phenotypic differentiation within *Macronycteris*.

Biogeographical considerations

Unfortunately, the lack of backbone support in the intron trees limits the biogeographical reconstructions possible with our analysis. The island of São Tomé appears to have been colonized once, fairly recently by an *M. gigas* lineage from western Africa, giving rise to the population of *M. thomensis* living there. The ML and BI phylogenies are equivocal about whether *M. cryptovalorona* and *M. commersonii* are sister species, raising the possibility that Madagascar has been colonized more than once. However, the intron trees suggest that

Downloaded from academic.oup.com/zoolinnean/article/207/4/zlag124/8770687 by guest on 27 August 2026

both *M. gigas* and the two Malagasy species have been derived from ancestral *M. vittata* populations, either as a clade (weakly indicated in the ML tree) or independently (BI tree). These inferred biogeographical events are consistent with the geographical range and habitat distributions of *Macronycteris* species (Supplementary Fig. S19). São Tomé Island lies ~255 km west of the coastal rainforests of Gabon inhabited by *M. gigas*. In contrast, *M. vittata* is associated primarily with woodland savanna habitats, although it may also occur in riparian forests. Its broad geographical distribution spans much of the latitudinal and longitudinal range of the genus *Macronycteris* and extends into Mozambique, the nearest mainland region to Madagascar. Future genomic research incorporating high-resolution datasets will be needed to resolve species relationships fully, particularly basal nodes, and to assess the evolutionary mechanisms driving differentiation in this bat clade.

Taxonomic implications

There were three comprehensive 20th century revisions of the family Hipposideridae: by Andersen (1905, 1906a, b), Tate (1941) and Hill (1963). The first recognized three species (*M. commersonii*, *M. gigas*, and *M. thomensis*), as did the second (*M. commersonii*, *M. gigas*, and *M. vittata*), whereas the third treated all named forms as conspecific. Despite the Eocene-aged divergence (timetree.org) of *Macronycteris* from its sister taxon *Doryrhina* (Foley *et al.* 2017; Patterson *et al.* 2020), mitochondrial and nuclear sequence analysis confirm the recent timing of splits within extant *Macronycteris*, dated by Foley *et al.* (2017) to the last 3 Myr. This timescale would explain the shallow divergences (<3%) among species in *Cytb* sequences and the incomplete lineage sorting observed in intron sequences. The latter is responsible for extensive paraphyly in phylogenetic analyses based on intron sequences (Foley *et al.* 2017; Patterson *et al.* 2020; Fig. 3). In contrast to the support for rapid diversification based on *Cytb* data in these two studies, Goodman *et al.* (2016) interpreted their *Cytb* data for *M. cryptovalorona* and *M. commersonii* as separating these species by 9%–11%. However, downloaded *Cytb* sequence data deposited in GenBank by Goodman *et al.* (2016) were incorporated in the study by Patterson *et al.* (2020) and in the present study, yielding an uncorrected *Cytb* distance of only 2.8% between *M. cryptovalorona* and *M. commersonii*. The basis for this discrepancy remains unclear, although the distance estimates reported by Goodman *et al.* (2016) differ substantially from those obtained by Rakotoarivelo *et al.* (2015), Patterson *et al.* (2020), and the present study.

Our integrative analyses provide variable support for the current recognition of five species within *Macronycteris*, while also highlighting important areas of uncertainty that warrant further investigation. The island endemic *M. thomensis* shows very limited genetic differentiation from West African *M. gigas* in our dataset, raising the possibility that it might represent a recently derived insular population rather than a fully distinct species. However, its marked differences in body size, morphology, geographical isolation, and echolocation calls, suggest that it is likely to be an independent evolutionary unit. Retaining *M. thomensis* as a distinct species is therefore justifiable under a lineage-based framework, although its status remains open to further testing. Although a monophyletic lineage comprising *M. gigas* from Kenya and the Central African Republic is as equidistant in our *Cytb* phylogeny as that of *M. thomensis*, there is no corroborating support for the evolutionary independence of this *M. gigas* clade in either morphological or acoustic data. In mainland Africa, the known distributions of both *M. gigas* and *M. vittata* are discontinuous and patchy (e.g. Burgin *et al.* 2020, and Supplementary Fig. S19). This complicates the application of names and led Monadjem (2019) to question whether the name *M. gigas*, coined in southern Angola, applies to the large *Macronycteris* of equatorial rainforests or whether the latter belong to a different, unrecognized taxon. Far better geographical sampling will be needed to address this, but both known mainland species occur in sympatry at Shimoni Cave, Kenya, supporting their specific distinction, despite limited genetic divergence. The specific distinction of *M. cryptovalorona* from *M. commersonii* in Madagascar can be challenged on the basis of their modest genetic and morphological differentiation. Known from only two sequenced specimens to date, *M. cryptovalorona* has been characterized incompletely, and its recognition as a separate species can be considered provisional pending further evidence from an increased sample size, particularly where the two forms have been cited to occur in sympatry (Goodman *et al.* 2016), and associated high-resolution genomic and integrative analyses. A comprehensive taxonomic revision integrating high-resolution genomic, morphological, and acoustic data will be necessary to clarify species boundaries and evolutionary relationships within this complex.

Morphology and echolocation

Morphology and species differentiation

Morphology plays an important role in species differentiation, particularly in bats, where skull shape is closely linked to diet, echolocation, and ecological adaptation. Our analyses revealed significant interspecific differences in external and cranial traits across *Macronycteris* species, with *M. gigas* exhibiting the largest dimensions and *M. thomensis* the smallest. Early field studies in Kenya documented clear differences between *M. gigas* and *M. vittata* in external morphology, craniodental traits, and echolocation calls (McWilliam 1982), and our results broadly agree with these observations. Interestingly, genetic analyses reveal the close relationships of this pair of species, underscoring the malleability of body size in this evolutionary radiation. The variation observed in skull shape and size among *Macronycteris* species is likely to reflect ecological adaptations relating to the size and hardness of their foods (Freeman 1981, Dumont 2007, Santana *et al.* 2011). The enormous sagittal crest and deep mandibular ramus of these bats, particularly in males, suggest that they can generate powerful bite forces, but no systematic study of their mastication has been conducted.

The significant influence of geography on morphology, particularly the smaller size of *M. commersonii*, *M. cryptovalorona*, *M. thomensis*, and the Bioko population of *M. gigas*, supports the hypothesis that insular dwarfism might have shaped their evolution. The significant difference

Downloaded from academic.oup.com/zoolinnean/article/207/4/zlag124/8770687 by guest on 27 August 2026

in FA and TTL between island and mainland species further aligns with classic cases of size reduction in insular mammal populations. Island populations often experience founder effects, resource limitation, relaxed competition and predation pressures, and other ecological pressures that can drive reductions in body size over evolutionary time (Lomolino 2005, Diniz-Filho *et al.* 2019, Benítez-López *et al.* 2021, Ponti *et al.* 2023). The islands of São Tomé and Príncipe provide striking examples of opposite patterns of size variation, even within populations still regarded as the same species, *Rousettus aegyptiacus*. On the smaller island of Príncipe, bats represent the smallest *R. aegyptiacus* found in Africa, whereas on São Tomé they form the largest lineage across the species range (Juste and Ibañez 1993, Rainho *et al.* 2022). Dietary niche breadth for most predators increases with body size, size enabling larger predators to detect and consume both small and large prey. However, Barclay and Brigham (1991) argued that the echolocation and flight systems of aerial insectivorous bats make smaller prey unavailable to larger bats, eliminating this advantage of larger body size.

The distribution of body sizes among *Macronycteris* species suggests patterns that are broadly consistent with the island rule, whereby larger-bodied species tend to become smaller on islands, whereas smaller-bodied species increase in size (Foster 1964). In a comprehensive review of changes in body size of bats on islands, Krzanowski (1967) documented 32 increases of body size in insular forms vs. 74 decreases, indicating a prevailing tendency towards smaller insular forms. However, a narrower survey by Meiri *et al.* (2008) found as many size increases as decreases among island bats, despite broad support for the rule in carnivorans, ungulates, and muroid rodents. More recently, Molinari (2023) used multiple measures of body size in bats and found discordant patterns among them, further questioning the generality of the rule in Chiroptera. Thus, the smaller body size of *Macronycteris* bats on islands in the Gulf of Guinea and Madagascar might not reflect a universal ecogeographical pattern but instead could result from lineage-specific ecological or evolutionary processes. For instance, it could simply reflect the lack of megafauna on those island systems and the smaller size (and perhaps lower resource availability) of the dung beetle faunas on these two islands that comprise an important part of the diet of *Macronycteris* spp. Smaller beetles would require smaller gape sizes and less powerful bite forces from the bats consuming them. In this regard, it should be considered that *M. gigas* shares the forests of mainland Africa with a larger set of other bats with similar foraging strategy and intermediate body size (the hipposiderid genera *Doryrhina* and *Hipposideros* and the rhinolophid *Rhinolophus*) that could compete for prey of intermediate size. Instead, *M. thomensis* shares the island of São Tomé with only one other species of bat with similar foraging strategy, the much smaller *Hipposideros* cf. *ruber* (Guillén-Servent *et al.* 1999). In the absence of species with intermediate body size, the ancestor of *M. thomensis* might have experienced an ecological release process that allowed a niche shift towards exploiting smaller prey, then evolving a smaller body size.

However, fossil evidence from Madagascar and beyond adds nuance to this interpretation. There is a well-documented fossil record of large-bodied hipposiderids (Gunnell and Simmons 2005). From the early Miocene of Australia (~16 Mya), several large genera have been described (e.g. Hand and Archer 2005), and many of these share close morphological similarities, particularly in tooth and cusp structure, with extant hipposiderids, suggesting relative stasis in dental morphology over millions of years. Recently, middle Miocene fossils from Madagascar, dated to ~10 Mya, have been described as a new genus and species, *Madanycteris razana* (Samonds *et al.* 2024). Although dentally similar to *Macronycteris*, *Madanycteris* is notably larger than any extant Malagasy species. Its classification as a new genus was based, in part, on the convention of not assigning such geologically ancient material to extant genera. In addition, *Hipposideros besaoka* (a large-bodied species from Late Pleistocene cave deposits in northwestern Madagascar, and probably best placed within *Macronycteris*) was smaller than *Madanycteris* but still larger than both *M. commersonii* and *M. cryptovalorona* (Samonds *et al.* 2024). These findings suggest that although the island rule predicts size reduction on islands, the size distribution seen today in Malagasy *Macronycteris* could also reflect the preferential extinction of larger-bodied species over time. Thus, the reduced body sizes observed in extant island populations of *Macronycteris* might not result solely from adaptive dwarfism. They might instead, or additionally, reflect extinction-driven filtering of the original size range, with larger forms, such as *H. besaoka*, disappearing within the last few thousand years. This raises the possibility that the island rule, at least in this context, might need to be reframed to account for extinction dynamics in addition to evolutionary change. Another possibility is that, given the considerable surface area of Madagascar (590000 km^2), it is too large and ecological diverse for the island rule to apply, in comparison to, for example, the smaller São Tomé (960 km^2).

Sexual dimorphism

Sexual dimorphism was also evident in cranial traits, with males generally exhibiting larger skull measurements than females across all five species. Sexual dimorphism is relatively rare in bats, where females are often larger than males (Myers 1978, Williams and Findley 1979). Instances where males are larger are typically associated with general polygyny or specifically lek mating systems (Bradbury 1977, McCracken and Bradbury 1977, Zeller 1984), but a number of studies have found no clear relationship between degree of polygyny and dimorphism, suggesting that sexual dimorphism is likely to be affected by multiple factors (Isaac 2005). Conversely, sexual segregation in bats is common and can be seen at roosts, in foraging, and in seasonal activity (Senior *et al.* 2005, Levin *et al.* 2013). Male-biased sexual dimorphism has been reported and studied in another hipposiderid, *Asellia tridens* (Jones *et al.* 1993). Amichai *et al.* (2013) found that male and female *A. tridens* differed in foraging patterns and in circadian rhythms during the warm months. These differences can lead to encounters with and responses to different selective factors,

Downloaded from academic.oup.com/zoolinnean/article/207/4/zlag124/8770687 by guest on 27 August 2026

suggesting that segregation, rather than mating system, might drive their dimorphism. Male and female *Macronycteris* bats are known to segregate seasonally at roosts and to migrate differentially to exploit seasonal eruptions of arthropod prey (Vaughan 1977, Cotterill and Fergusson 1999, Monadjem 2019). Ecological pressures arising from such differences might contribute to their sexual dimorphism. However, although ecological factors are likely to influence male and female behaviour and seasonal habitat use, our results suggest that these differences do not translate into population-level variation in cranial dimorphism. The fact that there is no significant interaction between sex and geography suggests that sexual dimorphism remains consistent in different environments, rather than being driven by local adaptations, perhaps attributable to different ontogenetic growth trajectories.

Although *Macronycteris* species exhibit striking sexual size dimorphism and differ in body size, they offer no support for Rensch's rule, which posits an increase in sexual size dimorphism with body size when males are the larger sex, but a decrease in dimorphism with size when females are larger (Fairbairn 1997). Previous examinations of this rule in bats used taxa generally exhibiting larger females: New World *Myotis* (Stevens and Platt 2015), *Rhinolophus* (Wu *et al.* 2014, 2018), and four families of Neotropical bats (Castillo-Figueroa 2024) all failed to support Rensch's rule. In our study (Table 3), each species exhibits significant male-biased sexual size dimorphism, but the degree of dimorphism fails to scale with size, with the largest species (*M. gigas*) intermediate in dimorphism and the smaller *M. vittata* exhibiting the greatest dimorphism. Although exceptions to the rule are supposedly uncommon and usually associated with female-biased size dimorphism (Fairbairn 1997), our test with *Macronycteris* shows that it also fails in instances of bats with male-biased dimorphism.

Echolocation call variation

The calls of hipposiderids consist of an initial constant-frequency element followed by a frequency-modulated sweep (Jones *et al.* 1993, Ramasindrazana *et al.* 2015, Webala *et al.* 2019). Like other rhinolophoids (i.e. Rhinolophidae and Rhinonycteridae), these calls are emitted through the nasal apparatus at high frequency. Given that their echolocation sequences contain a high proportion of sound vs. silence, the echolocation system is known as high duty cycle biosonar. Bats using this vocalization suite rely on Doppler-shift compensation to keep the frequency of the returning echoes within the narrow frequency range of the so-called 'acoustic fovea' (Schnitzler and Denzinger 2011). The 'acoustic fovea' is a region of the cochlea in the inner ears of the high duty cycle bats with a disproportionate length dedicated to the detection of wavelengths immediately flanking the characteristic frequency of the calls. This region makes possible the fine discrimination of the small frequency shifts caused in the echoes by the fluttering wings of insects that the bats use for prey classification (Schuller and Pollak 1979). This echolocation system is especially effective for exploiting prey flying in dense vegetation, because bats can separate echoes micro-modulated in amplitude and frequency from insects from the overlapping unmodulated echoes coming from the background acoustic clutter (Pavey *et al.* 2001, Fenton *et al.* 2012).

Dietary niche breadth increases with body size for most predators, size enabling larger predators to detect and consume both small and large prey. However, Barclay and Brigham (1991) argued that echolocation and flight systems of aerial insectivorous bats make small prey unavailable to large bats. Unlike most smaller hipposiderids, *Macronycteris* does not mainly rely on aerial foraging. *Macronycteris* species are known to forage from tree perches (Vaughan 1977), sallying out to intercept prey flying within 10 m and returning to the perch to consume it. By shifting from preying on small flying insects to larger arthropods, *Macronycteris* can more effectively use their lower-frequency calls, which do not attenuate as quickly as high-frequency calls. Dung beetles, a common prey of *Macronycteris* species, and other large arthropods are probably large enough to be detected and traced using low-frequency, low-repetition-rate calls and passive listening (Vaughan 1977).

Conclusion

In conclusion, our integrative assessment combining genetic, morphological, and bioacoustic data provides new insight into the evolutionary diversification of *Macronycteris*. Despite shallow mitochondrial divergence and limited resolution from nuclear introns, phenotypic and acoustic traits consistently distinguish the currently recognized species, supporting their taxonomic validity. These results illustrate how phenotypic and ecological divergence can arise rapidly in recently radiating lineages, even when genetic differentiation remains limited. By integrating multiple lines of evidence across the Afro-Malagasy distribution of the genus, this study provides a clearer taxonomic framework for *Macronycteris* and highlights the importance of combining molecular and phenotypic data to understand diversification in bats.

Acknowledgements

We are grateful to the many collectors and museum workers who helped to provide the resources on which this study was based. We are particularly grateful to Darrin Lunde and Megan Viera for loans of Smithsonian skeletal material, and to Bruno de Medeiros, Alfred Newton, and Gimo Daniel for insights concerning dung beetles. We also thank all funders and collaborators who made fieldwork and data collection possible for this work.

Author contributions

B.D.P. conceived the study. P.W.W., L.T., M.B., S.M.G., C.M., M.C.S., B.R., C.I., A.G-S., J.J., B.D.P. collected data. D.M.R., T.C.D. developed and performed the analytical and computational analyses. S.M.G., C.I., J.J., B.D.P. acquired funding. D.M.R., T.C.D., B.D.P. wrote the first draft of the manuscript, and all authors contributed to later drafts and discussion.

Downloaded from academic.oup.com/zoolinnean/article/207/4/zlag124/8770687 by guest on 27 August 2026

Supplementary material

Supplementary material is available at *Zoological Journal of the Linnean Society* online.

Conflicts of interest

None declared.

Funding

Collections in East and Southern Africa were funded by a variety of agencies in cooperation with the Field Museum, especially the JRS Biodiversity Foundation, Field Museum's Council on Africa, Marshall Field III Fund, Barbara E. Brown Fund for Mammal Research, and support from Bud and Onnolee Trapp.

Data availability

Data and R scripts are available in a GitHub repository (https://github.com/drossoni/Macronycteris).

References

Amador LI, Moyers Arévalo RL, Almeida FC *et al.* Bat systematics in the light of unconstrained analyses of a comprehensive molecular supermatrix. *Journal of Mammalian Evolution* 2018;**25**:37–70. https://doi.org/10.1007/s10914-016-9363-8

Amichai E, Levin E, Kronfeld-Schor N *et al.* Natural history, physiology and energetic strategies of *Asellia tridens* (Chiroptera). *Mammalian Biology* 2013;**78**:94–103. https://doi.org/10.1016/j.mambio.2012.06.006

Andersen K. On *Hipposiderus* [sic] *diadema* and its closest allies. *Annals & Magazine of Natural History* 1905;**16**:497–507. https://doi.org/10.1080/03745480509443077

Andersen K. On *Hipposiderus caffer*, Sund. and its closest allies; with some notes on *H. fuliginosus*, Temm. *Annals and Magazine of Natural History* 1906a;**17**:269–83. https://doi.org/10.1080/00222930608562523

Andersen K. On the bats of the *Hipposideros armiger* and *commersoni* types. *Annals & Magazine of Natural History* 1906b;**17**:35–48. https://doi.org/10.1080/00222930608562488

Arnold BD, Wilkinson GS. Female natal philopatry and gene flow between divergent clades of pallid bats (*Antrozous pallidus*). *Journal of Mammalogy* 2015;**96**:531–40. https://doi.org/10.1093/jmammal/gyv058

Barclay RMR, Brigham RM. Prey detection, dietary niche breadth, and body size in bats: why are aerial insectivorous bats so small? *The American Naturalist* 1991;**137**:693–703. https://doi.org/10.1086/285188

Benítez-López A, Santini L, Gallego-Zamorano J *et al.* The island rule explains consistent patterns of body size evolution across terrestrial vertebrates. *Nature Ecology & Evolution* 2021;**5**:768–86. https://doi.org/10.1038/s41559-021-01426-y

Bickham JW, Patton JC, Schlitter DA *et al.* Molecular phylogenetics, karyotypic diversity, and partition of the genus *Myotis* (Chiroptera: Vespertilionidae). *Molecular Phylogenetics and Evolution* 2004;**33**:333–8. https://doi.org/10.1016/j.ympev.2004.06.012

Bickham JW, Wood CC, Patton JC. Biogeographic implications of cytochrome *b* sequences and allozymes in sockeye (*Oncorhynchus nerka*). *The Journal of Heredity* 1995;**86**:140–4. https://doi.org/10.1093/oxfordjournals.jhered.a111544

Bonnet T, Leblois R, Rousset F *et al.* A reassessment of explanations for discordant introgressions of mitochondrial and nuclear genomes. *Evolution; International Journal of Organic Evolution* 2017;**71**:2140–58. https://doi.org/10.1111/evo.13296

Bouckaert R, Vaughan TG, Barido-Sottani J *et al.* BEAST 2.5: an advanced software platform for Bayesian evolutionary analysis. *PLoS Computational Biology* 2019;**15**:e1006650. https://doi.org/10.1371/journal.pcbi.1006650

Bradbury JW. Lek mating behavior in the hammer-headed bat. *Zeitschrift für Tierpsychologie* 1977;**45**:225–55. https://doi.org/10.1111/j.1439-0310.1977.tb02120.x

Bradley RD, Baker RJ. A test of the genetic species concept: cytochrome-*b* sequences and mammals. *Journal of Mammalogy* 2001;**82**:960–73. https://doi.org/10.1644/1545-1542(2001)082

Budinski I, Jojić V, Jovanović VM *et al.* Cranial variation of the greater horseshoe bat *Rhinolophus ferrumequinum* (Chiroptera: Rhinolophidae) from the central Balkans. *Zoologischer Anzeiger - A Journal of Comparative Zoology* 2015;**254**:8–14.

Burgin CJ, Wilson DE, Mittermeier RA *et al. Illustrated Checklist of the Mammals of the World. Vol.* **2**: *Eulipotyphla to Carnivora*. Barcelona: Lynx Edicions; 2020.

Castillo-Figueroa D. Sexual size dimorphism in 28 Neotropical bat species fails to obey Rensch's rule. *Acta Chiropterologica* 2024;**25**:311–21. https://doi.org/10.3161/15081109ACC2023.25.2.010

Cotterill FPD, Fergusson RA. Reproductive ecology of Commerson's leaf-nosed bats *Hipposideros commersoni* (Chiroptera: Hipposideridae) in south-central Africa: interactions between seasonality and large body size; and implications for conservation. *South African Journal of Zoology* 1999;**34**:53–63.

Degnan JH, Rosenberg NA. Gene tree discordance, phylogenetic inference and the multispecies coalescent. *Trends in Ecology & Evolution* 2009;**24**:332–40. https://doi.org/10.1016/j.tree.2009.01.009

Demos TC, Webala PW, Bartonjo M *et al.* Hidden diversity of African yellow house bats (Vespertilionidae, *Scotophilus*): insights from multilocus phylogenetics and lineage delimitation. *Frontiers in Ecology and Evolution* 2018;**6**:86. http://doi.org/10.3389/fevo.2018.00086

Denzinger A, Schnitzler H-U. Bat guilds, a concept to classify the highly diverse foraging and echolocation behaviors of microchiropteran bats. *Frontiers in Physiology* 2013;**4**:164. https://doi.org/10.3389/fphys.2013.00164

Diniz-Filho JAF, Jardim L, Rangel TF *et al.* Quantitative genetics of body size evolution on islands: an individual-based simulation approach. *Biology Letters* 2019;**15**:20190481. https://doi.org/10.1098/rsbl.2019.0481

Downloaded from academic.oup.com/zoolinnean/article/207/4/zlag124/8770687 by guest on 27 August 2026

Dumont ER. Feeding mechanisms in bats: variation within the constraints of flight. *Integrative and Comparative Biology* 2007;**47**:137–46. https://doi.org/10.1093/icb/icm007

Edgar RC. MUSCLE: multiple sequence alignment with high accuracy and high throughput. *Nucleic Acids Research* 2004;**32**:1792–7. https://doi.org/10.1093/nar/gkh340

Fairbairn DJ. Allometry for sexual size dimorphism: pattern and process in the coevolution of body size in males and females. *Annual Review of Ecology and Systematics* 1997;**28**:659–87. https://doi.org/10.1146/annurev.ecolsys.28.1.659

Fenton MB, Faure PA, Ratcliffe JM. Evolution of high duty cycle echolocation in bats. *The Journal of Experimental Biology* 2012;**215**:2935–44. http://doi.org/10.1242/jeb.073171

Flouri T, Jiao X, Rannala B *et al.* Species tree inference with BPP using genomic sequences and the multispecies coalescent. *Molecular Biology and Evolution* 2018;**35**:2585–93. https://doi.org/10.1093/molbev/msy147

Flouri T, Jiao X, Rannala B *et al.* A Bayesian implementation of the multispecies coalescent model with introgression for phylogenomic analysis. *Molecular Biology and Evolution* 2020;**37**:1211–23. https://doi.org/10.1093/molbev/msz296

Foley NM, Goodman SM, Whelan CV *et al.* Towards navigating the Minotaur's labyrinth: cryptic diversity and taxonomic revision within the speciose genus *Hipposideros* (Hipposideridae). *Acta Chiropterologica* 2017;**19**:1–18. http://doi.org/10.3161/15081109ACC2017.19.1.001

Foley NM, Thong VD, Soisook P *et al.* How and why overcome the impediments to resolution: lessons from rhinolophid and hipposiderid bats. *Molecular Biology and Evolution* 2015;**32**:313–33. http://doi.org/10.1093/molbev/msu329

Foster JB. Evolution of mammals on islands. *Nature* 1964;**202**:234–5. https://doi.org/10.1038/202234a0

Freeman PW. Correspondance of food habits and morphology in insectivorous bats. *Journal of Mammalogy* 1981;**62**:166–73. https://doi.org/10.2307/1380489dumont

Fujisawa T, Barraclough TG. Delimiting species using single-locus data and the Generalized Mixed Yule Coalescent approach: a revised method and evaluation on simulated data sets. *Systematic Biology* 2013;**62**:707–24. https://doi.org/10.1093/sysbio/syt033

Funk WC, McKay JK, Hohenlohe PA *et al.* Harnessing genomics for delineating conservation units. *Trends in Ecology & Evolution* 2012;**27**:489–96. https://doi.org/10.1016/j.tree.2012.05.012

Furman A, Çoraman E, Çelik YE *et al.* Cytonuclear discordance and the species status of *Myotis myotis* and *Myotis blythii* (Chiroptera). *Zoologica Scripta* 2014;**43**:549–61. https://doi.org/10.1111/zsc.12076

Goodman SM, Ramasindrazana B. *Chauves-souris ou ordre des Chiroptera/ Bats or the Order Chiroptera. Dans Atlas d'une sélection de vertébrés terrestres de Madagascar/ Atlas of Selected Land Vertebrates of Madagascar*. Goodman SM, Raherilalao MJ (eds.). Antananarivo: Association Vahatra, 2013, 169–209.

Goodman SM, Schoeman MC, Rakotoarivelo A *et al.* How many species of *Hipposideros* have occurred on Madagascar since the Late Pleistocene? *Zoological Journal of the Linnean Society* 2016;**177**:428–49. https://doi.org/10.1111/zoj.12368

Guillén-Servent A, Juste B, Ibáñez C. Variation in the frequency of the echolocation calls of *Hipposideros ruber* in the Gulf of Guinea: an exploration of the adaptive meaning of the constant frequency value in rhinolophoid CF bats. *Journal of Evolutionary Biology* 1999;**13**:70–80. https://doi.org/10.1046/j.1420-9101.2000.00155.x

Gunnell GF, Simmons NB. Fossil evidence and the origin of bats. *Journal of Mammalian Evolution* 2005;**12**:209–46. https://doi.org/10.1007/s10914-005-6945-2

Gutiérrez-Guerrero Y, Ibarra-Laclette E, Martínez del Río C *et al.* Genomic consequences of dietary diversification and parallel evolution due to nectarivory in leaf-nosed bats. *GigaScience* 2020;**9**:giaa059. https://doi.org/10.1093/gigascience/giaa059

Hand SJ, Archer M. A new hipposiderid genus (Microchiroptera) from an Early Miocene bat community in Australia. *Palaeontology* 2005;**48**:371–83. https://doi.org/10.1111/j.1475-4983.2005.00444.x

Happold M. Genus *Hipposideros*: Old World leaf-nosed bats. In: Happold M, Happold DCD (eds.), *The Mammals of Africa, Vol. 4: Hedgehogs, Shrews and Bats*. London: Bloomsbury, 2013, 367–71. https://doi.org/10.5040/9781472926944.part-0035

Hartley DJ. Stabilization of perceived echo amplitudes in echolocating bats. I. Echo detection and automatic gain control in the big brown bat, *Eptesicus fuscus*, and the fishing bat, *Noctilio leporinus*. *The Journal of the Acoustical Society of America* 1992;**91**:1120–32. https://doi.org/10.1121/1.402639

Heller K-G, Helversen O. Resource partitioning of sonar frequency bands in rhinolophoid bats. *Oecologia* 1989; **80**:178–86.

Hill JE. A revision of the genus *Hipposideros*. *Bulletin of the British Museum (Natural History) Zoology* 1963;**11**:1–129. https://www.biodiversitylibrary.org/page/2340907

Hiryu S, Mora EC, Riquimaroux H. Behavioral and physiological bases for Doppler shift compensation by echolocating bats. In: Fenton MB, Grinnell A, Popper A *et al.* (eds.), *Bat Bioacoustics, Springer Handbook of Auditory Research*, Vol. **54**. New York, NY: Springer, 2016, 239–63. https://doi.org/10.1007/978-1-4939-3527-7_9

Igea J, Juste J, Castresana J. Novel intron markers to study the phylogeny of closely related mammalian species. *BMC Evolutionary Biology* 2010;**10**:369. https://doi.org/10.1186/1471-2148-10-369

Isaac JL. Potential causes and life-history consequences of sexual size dimorphism in mammals. *Mammal Review* 2005; **35**:101–15. https://doi.org/10.1111/j.1365-2907.2005.00045.x

Jacobs DS, Catto S, Mutumi GL *et al.* Testing the sensory drive hypothesis: geographic variation in echolocation frequencies of Geoffroy's horseshoe bat (Rhinolophidae: *Rhinolophus clivosus*). *PLoS One* 2017;**12**:e0187769. https://doi.org/10.1371/journal.pone.0187769

Jones G, Holderied MW. Bat echolocation calls: adaptation and convergent evolution. *Proceedings of the Royal Society B: Biological Sciences* 2007;**274**:905–12. https://doi.org/10.1098/rspb.2006.0200

Downloaded from academic.oup.com/zoolinnean/article/207/4/zlag124/8770687 by guest on 27 August 2026

Jones G, Morton M, Hughes PM *et al.* Echolocation, flight morphology and foraging strategies of some West African hipposiderid bats. *Journal of Zoology* 1993;**230**:385–400. https://doi.org/10.1111/j.1469-7998.1993.tb02691.x

Jung K, Molinari J, Kalko EKV. Driving factors for the evolution of species-specific echolocation call design in New World free-tailed bats (Molossidae). *PLoS One* 2014;**9**:e85279. https://dx.doi.org/10.1371/journal.pone.0085279

Juste J, Ibañez C. Geographic variation and taxonomy of *Rousettus aegyptiacus* (Mammalia: Megachiroptera) in the islands of the Gulf of Guinea. *Zoological Journal of the Linnean Society* 1993; **107**:117–29. https://doi.org/10.1111/j.1096-3642.1993.tb00217.x

Kapli P, Lutteropp S, Zhang J *et al.* Multi-rate Poisson tree processes for single-locus species delimitation under maximum likelihood and Markov chain Monte Carlo. *Bioinformatics (Oxford, England)* 2017;**33**:1630–8. https://doi.org/10.1093/bioinformatics/btx025

Krzanowski A. The magnitude of islands and the size of bats (Chiroptera). *Acta Zoologica Cracoviensia* 1967;**12**:281–348. http://isez.pan.krakow.pl/journals/azc/pdf/12/12_11.pdf

Kumar S, Stecher G, Suleski M *et al.* TimeTree: a resource for timelines, timetrees, and divergence times. *Molecular Biology and Evolution* 2017;**34**:1812–9. https://doi.org/10.1093/molbev/msx116

Kumar S, Stecher G, Suleski M *et al.* MEGA12: Molecular Evolutionary Genetic Analysis version 12 for adaptive and green computing. *Molecular Biology and Evolution* 2024; **41**:msae263. https://doi.org/10.1093/molbev/msae263

Leigh JW, Bryant D. POPART: full-feature software for haplotype network construction. *Methods in Ecology and Evolution* 2015; **6**:1110–6. https://doi.org/10.1111/2041-210X.12410

Levin E, Roll U, Dolev A *et al.* Bats of a gender flock together: sexual segregation in a subtropical bat. *PLoS One* 2013; **8**:e54987. https://doi.org/10.1371/journal.pone.0054987

Lomolino MV. Body size evolution in insular vertebrates: generality of the island rule. *Journal of Biogeography* 2005; **32**:1683–99. https://doi.org/10.1111/j.1365-2699.2005.01314.x

Lopes F, Oliveira LR, Kessler A *et al.* Phylogenomic discordance in the eared seals is best explained by incomplete lineage sorting following explosive radiation in the Southern Hemisphere. *Systematic Biology* 2021;**70**:786–802. https://doi.org/10.1093/sysbio/syaa099

Maddison WP, Knowles LL. Inferring phylogeny despite incomplete lineage sorting. *Systematic Biology* 2006;**55**:21–30. https://doi.org/10.1080/10635150500354928

Mallet J. Hybridization as an invasion of the genome. *Trends in Ecology & Evolution* 2005;**20**:229–37. https://doi.org/10.1016/j.tree.2005.02.010

Mammal Diversity Database. American Society of Mammalogists, 2024. www.mammaldiversity.org.

Mao X, Tsagkogeorga G, Bailey SE *et al.* Genomics of introgression in the Chinese horseshoe bat (*Rhinolophus sinicus*) revealed by transcriptome sequencing. *Biological Journal of the Linnean Society* 2017;**121**:698–710. http://doi.org/10.1093/biolinnean/blx017

Marr MM, Hopkins K, Tapley B *et al.* What's in a name? Using species delimitation to inform conservation practice for Chinese giant salamanders (*Andrias* spp.). *Evolutionary Journal of the Linnean Society* 2024;**3**:kzae007. https://doi.org/10.1093/evolinnean/kzae007

Matthee CA, Burzlaff JD, Taylor JF *et al.* Mining the mammalian genome for artiodactyl systematics. *Systematic Biology* 2001;**50**:367–90.https://doi.org/10.1080/10635150119683

McCracken GF, Bradbury JW. Paternity and genetic heterogeneity in the polygynous bat, *Phyllostomus hastatus*. *Science (New York, N.Y.)* 1977;**198**:303–6. https://doi.org/10.1126/science.198.4314.303

McWilliam A. Adaptive responses to seasonality in four species of *Microchiroptera* in coastal Kenya. Unpublished PhD thesis, University of Aberdeen, Aberdeen, UK, 1982.

Meiri S, Cooper N, Purvis A. The island rule: made to be broken? *Proceedings. Biological Sciences* 2008;**275**:141–8. https://doi.org/10.1098/rspb.2007.1056

Miller MA, Pfeiffer W, Schwartz T. Creating the CIPRES Science Gateway for inference of large phylogenetic trees. Gateway Computing Environments Workshop (GCE). New Orleans, LA: IEEE, 2010. http://dx.doi.org/10.1109/GCE.2010.5676129

Minh BQ, Schmidt HA, Chernomor O *et al.* IQ-TREE 2: new models and efficient methods for phylogenetic inference in the genomic era. *Molecular Biology and Evolution* 2020;**37**:1530–4. https://doi.org/10.1093/molbev/msaa015

Missagia RV, Patterson BD, Perini FA. Stable isotope signatures and the trophic diversification of akodontine rodents. *Evolutionary Ecology* 2019;**33**:855–72. https://doi.org/10.1007/s10682-019-10009-0

Moir HM, Jackson JC, Windmill JF. Extremely high frequency sensitivity in a 'simple' ear. *Biology Letters* 2013;**9**:20130241. https://doi.org/10.1098/rsbl.2013.0241

Molinari J. A global assessment of the 'island rule' in bats based on functionally distinct measures of body size. *Journal of Biogeography* 2023;**50**:1179–90. https://doi.org/10.1111/jbi.14624

Monadjem A. Family Hipposideridae (Old World leaf-nosed bats). In: Wilson DE, Mittermeier RA (eds.), *Handbook of the Mammals of the World, Vol. 9. Bats*. Barcelona: Lynx Ediciones, 2019, 210–27.

Monadjem A, Montauban C, Webala PW *et al.* African bat database: curated data of occurrences, distributions and conservation metrics for sub-Saharan bats. *Scientific Data* 2024; **11**:1309. https://doi.org/10.1038/s41597-024-04170-7

Monadjem A, Richards L, Taylor PJ *et al.* Diversity of Hipposideridae in the Mount Nimba massif, West Africa, and the taxonomic status of *Hipposideros lamottei*. *Acta Chiropterologica* 2013;**15**:341–52. https://doi.org/10.3161/150811013X678964

Morales AE, Carstens BC. Evidence that *Myotis lucifugus* 'subspecies' are five non-sister species, despite gene flow. *Systematic Biology* 2018;**67**:756–69. https://doi.org/10.1093/sysbio/syy010

Myers P. Sexual dimorphism in size of vespertilionid bats. *The American Naturalist* 1978;**112**:701–11. https://doi.org/10.1086/283312

Naidoo T, Schoeman MC, Goodman SM *et al.* Discordance between mitochondrial and nuclear genetic structure in the bat *Chaerephon pumilus* (Chiroptera: Molossidae) from

Downloaded from academic.oup.com/zoolinnean/article/207/4/zlag124/8770687 by guest on 27 August 2026

southern Africa. *Mammalian Biology* 2016;**81**:115–22. http://dx.doi.org/10.1016/j.mambio.2015.11.002

Nosil P, Funk DJ, Ortiz-Barrientos D. Divergent selection and heterogeneous genomic divergence. *Molecular Ecology* 2009; **18**:375–402. https://doi.org/10.1111/j.1365-294X.2008.03946.x

Ospina-Garcés SM, De Luna E, Herrera MLG *et al.* Cranial shape and diet variation in *Myotis* species (Chiroptera: Vespertilionidae): testing the relationship between form and function. *Acta Chiropterologica* 2016;**18**:163–80.

Patterson BD, Webala PW, Lavery T *et al.* Evolutionary relationships and population genetics of the Afrotropical leaf-nosed bats (Chiroptera: Hipposideridae). *ZooKeys* 2020;**929**:117–61. http://doi.org/10.3897/zookeys.929.50240

Pavey CR, Grunwald JE, Neuweiler G. Foraging habitat and echolocation behaviour of Schneider's leaf nosed bat, *Hipposideros speoris*, in a vegetation mosaic in Sri Lanka. *Behavioral Ecology and Sociobiology* 2001;**50**:209–18. https://doi.org/10.1007/s002650100363

Peters WCH. Über die Gattungen und Arten der Hufeisennasen, *Rhinolophi*. *Monatsberichte der Königlichen Preussischen Akademie der Wissenschaften zu Berlin* 1871;**1871**:301–32. https://www.biodiversitylibrary.org/bibliography/48522

Petit RJ, Excoffier L. Gene flow and species delimitation. *Trends in Ecology & Evolution* 2009;**24**:386–93. https://doi.org/10.1016/j.tree.2009.02.011

Ponti R, Doutrelant C, Covas R. Strength of the 'island rule' in birds is positively associated with absence of avian predators. *Biology Letters* 2023;**19**:20220536. https://doi.org/10.1098/rsbl.2022.0536

Puechmaille SJ, Borissov IM, Zsebok S *et al.* Female mate choice can drive the evolution of high frequency echolocation in bats: a case study with *Rhinolophus mehelyi*. *PLoS One* 2014;**9**:e103452. https://doi.org/10.1371/journal.pone.0103452.

Pye JD. A theory of echolocation by bats. *The Journal of Laryngology and Otology* 1960;**74**:718–29. https://doi.org/10.1017/S0022215100057170

Rainho A, Meyer CFJ, Thorsteinsdóttir S *et al.* Current knowledge and conservation of the wild mammals of the Gulf of Guinea Oceanic Islands. In: Ceríaco LMP, de Lima RF, Melo M *et al.* (eds.) *Biodiversity of the Gulf of Guinea Oceanic Islands*. Cham: Springer, 2022, 593–619. https://doi.org/10.1007/978-3-031-06153-0_22

Rakotoarivelo A, Goodman SM, Schoeman MC *et al.* Phylogeography and population genetics of *Macronycteris commersonii* s.s. (Chiroptera: Hipposideridae), an endemic Malagasy bat. *PeerJ* 2019;**7**:e5866. https://doi.org/10.7717/peerj.5866

Rakotoarivelo A, Ralisata M, Ravoahangimalala OR *et al.* The food habits of a Malagasy giant: *Hipposideros commersoni* (E. Geoffroy, 1813). *African Journal of Ecology* 2009;**47**:283–8.

Rakotoarivelo AR, Willows-Munro S, Schoeman MC *et al.* Cryptic diversity in *Hipposideros commersoni* sensu stricto (Chiroptera: Hipposideridae) in the western portion of Madagascar. *BMC Evolutionary Biology* 2015;**15**:235. https://doi.org/10.1186/s12862-015-0510-2 26518602

Ramasindrazana B, Rakotondramanana FC, Schoeman CM *et al.* Evidence of echolocation call divergence in *Hipposideros commersoni* sensu stricto (E. Geoffroy, 1803) from Madagascar and correlation with body size. *Acta Chiropterologica* 2015;**17**:85–94.

R Core Team. *R: A Language and Environment for Statistical Computing*. Vienna, Austria: R Foundation for Statistical Computing; 2025.

Rambaut A, Drummond AJ, Xie D *et al.* Posterior summarization in Bayesian phylogenetics using Tracer 1.7. *Systematic Biology* 2018;**67**:901–4. https://doi.org/10.1093/sysbio/syy032

Rannala B, Yang Z. Improved reversible jump algorithms for Bayesian species delimitation. *Genetics* 2013;**194**:245–53. https://doi.org/10.1534/genetics.112.149039

Rannala B, Yang Z. Efficient Bayesian species tree inference under the multispecies coalescent. *Systematic Biology* 2017;**66**:823–42. https://doi.org/10.1093/sysbio/syw119

Ronquist F, Teslenko M, van der Mark P *et al.* MrBayes 3.2: efficient Bayesian phylogenetic inference and model choice across a large model space. *Systematic Biology* 2012;**61**:539–42. https://dx.doi.org/10.1093/sysbio/sys029

Rossoni DM, Assis APA, Giannini NP *et al.* Intense natural selection preceded the invasion of new adaptive zones during the radiation of New World leaf-nosed bats. *Scientific Reports* 2017;**7**:11076. https://doi.org/10.1038/s41598-017-08989-6

Rossoni DM, Costa BM, Giannini NP *et al.* A multiple peak adaptive landscape based on feeding strategies and roosting ecology shaped the evolution of cranial covariance structure and morphological differentiation in phyllostomid bats. *Evolution; International Journal of Organic Evolution* 2019;**73**:961–81. https://doi.org/10.1111/evo.13715

Salicini I, Ibáñez C, Juste J. Multilocus phylogeny and species delimitation within the Natterer's bat species complex in the Western Palearctic. *Molecular Phylogenetics and Evolution* 2011;**61**:888–98. https://doi.org/10.1016/j.ympev.2011.08.010

Samonds KE, Simmons NB, Goodman SM *et al.* Oldest record of Cenozoic terrestrial vertebrates (Chiroptera) from Madagascar. *Journal of Vertebrate Paleontology* 2024;**44**:e2488447. https://doi.org/10.1080/02724634.2025.2488447

Santana SE, Cheung E. Go big or go fish: morphological specializations in carnivorous bats. *Proceedings. Biological Sciences* 2016;**283**:20160615. https://doi.org/10.1098/rspb.2016.0615

Santana SE, Strait S, Dumont ER. The better to eat you with: functional correlates of tooth structure in bats. *Functional Ecology* 2011;**25**:839–47. https://doi.org/10.1111/j.1365-2435.2011.01832.x

Schnitzler H-U, Denzinger A. Auditory fovea and Doppler shift compensation: adaptations for flutter detection in echolocating bats using CF-FM signals. *Journal of Comparative Physiology. A, Neuroethology, Sensory, Neural, and Behavioral Physiology* 2011;**197**:541–59. https://doi.org/10.1007/s00359-010-0569-6

Schnitzler H-U, Kalko EKV. Echolocation by insect-eating bats. *BioScience* 2001;**51**:557–69. https://doi.org/10.1641/0006-3568(2001)051[0557: EBIEB]2.0.CO; 2

Downloaded from academic.oup.com/zoolinnean/article/207/4/zlag124/8770687 by guest on 27 August 2026

Schuller G, Pollak G. Disproportionate frequency representation in the inferior colliculus of Doppler-compensating greater horseshoe bats: evidence for an acoustic fovea. *Journal of Comparative Physiology. A, Neuroethology, Sensory, Neural, and Behavioral Physiology* 1979;**132**:47–54. https://doi.org/10.1007/BF00617731

Senior P, Butlin RK, Altringham JD. Sex and segregation in temperate bats. *Proceedings of the Royal Society B: Biological Sciences* 2005;**272**:2467–73. https://doi.org/10.1098/rspb.2005.3237

Simmons NB. Chiroptera. In: Wilson DE, Reeder DAM (eds.), *Mammal Species of the World: A Taxonomic and Geographic Reference*, 3rd edn. Baltimore, MD: Johns Hopkins University Press, 2005, 312–529.

Stevens RD, Platt RN. Patterns of secondary sexual size dimorphism in New World *Myotis* and a test of Rensch's rule. *Journal of Mammalogy* 2015;**96**:1128–34. https://doi.org/10.1093/jmammal/gyv120

Suchard MA, Lemey P, Baele G *et al.* Bayesian phylogenetic and phylodynamic data integration using BEAST 1.10. *Virus Evolution* 2018;**4**:vey016. https://doi.org/10.1093/ve/vey016

Toews DP, Brelsford A. The biogeography of mitochondrial and nuclear discordance in animals. *Molecular Ecology* 2012;**21**:3907–30. http://doi.org/10.1111/j.1365-294X.2012.05664.x

Tomasco IH, Giorello FM, Boullosa N *et al.* The contribution of incomplete lineage sorting and introgression to the evolutionary history of the fast-evolving genus *Ctenomys* (Rodentia, Ctenomyidae). *Molecular Phylogenetics and Evolution* 2022;**176**:107593. https://doi.org/10.1016/j.ympev.2022.107593

Tuneu-Corral C, Puig-Montserrat X, Flaquer C *et al.* Landscape of fear in rice paddies: effect of bat ultrasounds on the egg production of a tympanate moth pest. *Pest Management Science* 2025;**81**:5114–22. https://doi.org/10.1002/ps.8866

Vaughan TA. Foraging behaviour of the giant leaf-nosed bat (*Hipposideros commersoni*). *African Journal of Ecology* 1977;**15**:237–49. https://doi.org/10.1111/j.1365-2028.1977.tb00406.x

Velazco PM, Gardner AL. A new species of *Lophostoma* d'Orbigny, 1836 (Chiroptera: Phyllostomidae) from Panama. *Journal of Mammalogy* 2012;**93**:605–14. http://doi.org/10.1644/11-MAMM-A-217.1

Webala PW, Rydell J, Dick CW *et al.* Echolocation calls of high duty-cycle bats (Hipposideridae and Rhinonycteridae) from Kenya. *Journal of Bat Research & Conservation* 2019;**12**:10–20. http://hdl.handle.net/123456789/8945

Williams DF, Findley JS. Sexual size dimorphism in vespertilionid bats. *American Midland Naturalist* 1979;**102**:113–26. https://doi.org/10.2307/2425072

Wu H, Jiang T, Huang X *et al.* A test of Rensch's rule in greater horseshoe bat (*Rhinolophus ferrumequinum*) with female-biased sexual size dimorphism. *PLoS One* 2014;**9**:e86085. https://doi.org/10.1371/journal.pone.0086085

Wu H, Jiang T, Huang X *et al.* Patterns of sexual size dimorphism in horseshoe bats: testing Rensch's rule and potential causes. *Scientific Reports* 2018;**8**:2616. https://doi.org/10.1038/s41598-018-21077-7

Yang Z. The BPP program for species tree estimation and species delimitation. *Current Zoology* 2015;**61**:854–65. https://doi.org/10.1093/czoolo/61.5.854

Yang Z, Rannala B. Bayesian species delimitation using multilocus sequence data. *Proceedings of the National Academy of Sciences of the United States of America* 2010;**107**:9264–9. https://doi.org/10.1073/pnas.091302210

Yang Z, Rannala B. Unguided species delimitation using DNA sequence data from multiple loci. *Molecular Biology and Evolution* 2014;**31**:3125–35. https://doi.org/10.1093/molbev/msu279

Zeller U. Zur Kenntnis des Stimmapparates der Epauletten-Flughunde. *Zeitschrift für Säugetierkunde* 1984;**49**:207–20. http://pascal-francis.inist.fr/vibad/index.php?action=getRecordDetail&idt=8910272

Downloaded from academic.oup.com/zoolinnean/article/207/4/zlag124/8770687 by guest on 27 August 2026

© The Author(s) 2026. Published by Oxford University Press on behalf of The Linnean Society of London.
This is an Open Access article distributed under the terms of the Creative Commons Attribution License (https://creativecommons.org/licenses/by/4.0/), which permits unrestricted reuse, distribution, and reproduction in any medium, provided the original work is properly cited. Zoological Journal of the Linnean Society 2026 207(4) 1–26
https://doi.org/10.1093/zoolinnean/zlag124
Original Article